

FILE COPY  
NO. **2**

**★** CASE FILE #2  
COPY

# NATIONAL ADVISORY COMMITTEE FOR AERONAUTICS

REPORT No. 594

## CHARACTERISTICS OF SIX PROPELLERS INCLUDING THE HIGH-SPEED RANGE

By THEODORE THEODORSEN, GEORGE W. STICKLE  
and M. J. BREVOORT



THIS DOCUMENT ON LOAN FROM THE FILES OF

NATIONAL ADVISORY COMMITTEE FOR AERONAUTICS  
LANGLEY AERONAUTICAL LABORATORY  
LANGLEY FIELD, HAMPTON, VIRGINIA

RETURN TO THE ABOVE ADDRESS.

REQUESTS FOR PUBLICATIONS SHOULD BE ADDRESSED  
AS FOLLOWS:

NATIONAL ADVISORY COMMITTEE FOR AERONAUTICS  
1724 F STREET, N.W.,  
WASHINGTON 25, D.C.

1937

## AERONAUTIC SYMBOLS

### 1. FUNDAMENTAL AND DERIVED UNITS

	Symbol	Metric		English	
		Unit	Abbrevia- tion	Unit	Abbrevia- tion
Length.....	$l$	meter.....	m	foot (or mile).....	ft. (or mi.)
Time.....	$t$	second.....	s	second (or hour).....	sec. (or hr.)
Force.....	$F$	weight of 1 kilogram.....	kg	weight of 1 pound.....	lb.
Power.....	$P$	horsepower (metric).....		horsepower.....	hp.
Speed.....	$V$	{kilometers per hour.....	k.p.h.	miles per hour.....	m.p.h.
		{meters per second.....	m.p.s.	feet per second.....	f.p.s.

### 2. GENERAL SYMBOLS

<p><math>W</math>, Weight = <math>mg</math></p> <p><math>g</math>, Standard acceleration of gravity = 9.80665 m/s<sup>2</sup> or 32.1740 ft./sec.<sup>2</sup></p> <p><math>m</math>, Mass = <math>\frac{W}{g}</math></p> <p><math>I</math>, Moment of inertia = <math>mk^2</math>. (Indicate axis of radius of gyration <math>k</math> by proper subscript.)</p> <p><math>\mu</math>, Coefficient of viscosity</p>	<p><math>\nu</math>, Kinematic viscosity</p> <p><math>\rho</math>, Density (mass per unit volume)</p> <p>Standard density of dry air, 0.12497 kg-m<sup>-4</sup>-s<sup>2</sup> at 15° C. and 760 mm; or 0.002378 lb.-ft.<sup>-4</sup> sec.<sup>2</sup></p> <p>Specific weight of "standard" air, 1.2255 kg/m<sup>3</sup> or 0.07651 lb./cu. ft.</p>
--	--

### 3. AERODYNAMIC SYMBOLS

<p><math>S</math>, Area</p> <p><math>S_w</math>, Area of wing</p> <p><math>G</math>, Gap</p> <p><math>b</math>, Span</p> <p><math>c</math>, Chord</p> <p><math>\frac{b^2}{S}</math>, Aspect ratio</p> <p><math>V</math>, True air speed</p> <p><math>q</math>, Dynamic pressure = <math>\frac{1}{2}\rho V^2</math></p> <p><math>L</math>, Lift, absolute coefficient <math>C_L = \frac{L}{qS}</math></p> <p><math>D</math>, Drag, absolute coefficient <math>C_D = \frac{D}{qS}</math></p> <p><math>D_0</math>, Profile drag, absolute coefficient <math>C_{D_0} = \frac{D_0}{qS}</math></p> <p><math>D_i</math>, Induced drag, absolute coefficient <math>C_{D_i} = \frac{D_i}{qS}</math></p> <p><math>D_p</math>, Parasite drag, absolute coefficient <math>C_{D_p} = \frac{D_p}{qS}</math></p> <p><math>C</math>, Cross-wind force, absolute coefficient <math>C_C = \frac{C}{qS}</math></p> <p><math>R</math>, Resultant force</p>	<p><math>i_w</math>, Angle of setting of wings (relative to thrust line)</p> <p><math>i_t</math>, Angle of stabilizer setting (relative to thrust line)</p> <p><math>Q</math>, Resultant moment</p> <p><math>\Omega</math>, Resultant angular velocity</p> <p><math>\rho \frac{Vl}{\mu}</math>, Reynolds Number, where <math>l</math> is a linear dimension (e.g., for a model airfoil 3 in. chord, 100 m.p.h. normal pressure at 15° C., the corresponding number is 234,000; or for a model of 10 cm chord, 40 m.p.s., the corresponding number is 274,000)</p> <p><math>C_p</math>, Center-of-pressure coefficient (ratio of distance of c.p. from leading edge to chord length)</p> <p><math>\alpha</math>, Angle of attack</p> <p><math>\epsilon</math>, Angle of downwash</p> <p><math>\alpha_0</math>, Angle of attack, infinite aspect ratio</p> <p><math>\alpha_i</math>, Angle of attack, induced</p> <p><math>\alpha_a</math>, Angle of attack, absolute (measured from zero-lift position)</p> <p><math>\gamma</math>, Flight-path angle</p>
--	--

---

---

**REPORT No. 594**

---

**CHARACTERISTICS OF SIX PROPELLERS INCLUDING  
THE HIGH-SPEED RANGE**

By **THEODORE THEODORSEN, GEORGE W. STICKLE**  
and **M. J. BREVOORT**

**Langley Memorial Aeronautical Laboratory**

---

---

I

## NATIONAL ADVISORY COMMITTEE FOR AERONAUTICS

HEADQUARTERS, NAVY BUILDING, WASHINGTON, D. C.

LABORATORIES, LANGLEY FIELD, VA.

Created by act of Congress approved March 3, 1915, for the supervision and direction of the scientific study of the problems of flight (U. S. Code, Title 50, Sec. 151). Its membership was increased to 15 by act approved March 2, 1929. The members are appointed by the President, and serve as such without compensation.

JOSEPH S. AMES, Ph. D., *Chairman*,  
Baltimore, Md.

DAVID W. TAYLOR, D. Eng., *Vice Chairman*,  
Washington, D. C.

WILLIS RAY GREGG, Sc. D., *Chairman, Executive Committee*,  
Chief, United States Weather Bureau.

CHARLES G. ABBOT, Sc. D.,  
Secretary, Smithsonian Institution.

LYMAN J. BRIGGS, Ph. D.,  
Director, National Bureau of Standards.

ARTHUR B. COOK, Rear Admiral, United States Navy,  
Chief, Bureau of Aeronautics, Navy Department.

FRED D. FAGG, JR., J. D.,  
Director of Air Commerce, Department of Commerce.

HARRY F. GUGGENHEIM, M. A.,  
Port Washington, Long Island, N. Y.

SYDNEY M. KRAUS, Captain, United States Navy,  
Bureau of Aeronautics, Navy Department.

CHARLES A. LINDBERGH, LL. D.,  
New York City.

WILLIAM P. MACCRACKEN, J. D.,  
Washington, D. C.

AUGUSTINE W. ROBINS, Brigadier General, United States  
Army,  
Chief Matériel Division, Air Corps, Wright Field, Day-  
ton, Ohio.

EDWARD P. WARNER, M. S.,  
Greenwich, Conn.

OSCAR WESTOVER, Major General, United States Army,  
Chief of Air Corps, War Department.

ORVILLE WRIGHT, Sc. D.,  
Dayton, Ohio.

GEORGE W. LEWIS, *Director of Aeronautical Research*

JOHN F. VICTORY, *Secretary*

HENRY J. E. REID, *Engineer in Charge, Langley Memorial Aeronautical Laboratory, Langley Field, Va.*

JOHN J. IDE, *Technical Assistant in Europe, Paris, France*

### TECHNICAL COMMITTEES

AERODYNAMICS  
POWER PLANTS FOR AIRCRAFT  
AIRCRAFT MATERIALS

AIRCRAFT STRUCTURES  
AIRCRAFT ACCIDENTS  
INVENTIONS AND DESIGNS

*Coordination of Research Needs of Military and Civil Aviation*

*Preparation of Research Programs*

*Allocation of Problems*

*Prevention of Duplication*

*Consideration of Inventions*

### LANGLEY MEMORIAL AERONAUTICAL LABORATORY

LANGLEY FIELD, VA.

Unified conduct, for all agencies, of  
scientific research on the fundamental  
problems of flight.

### OFFICE OF AERONAUTICAL INTELLIGENCE

WASHINGTON, D. C.

Collection, classification, compilation,  
and dissemination of scientific and tech-  
nical information on aeronautics.

## REPORT No. 594

### CHARACTERISTICS OF SIX PROPELLERS INCLUDING THE HIGH-SPEED RANGE

By THEODORE THEODORSEN, GEORGE W. STICKLE, and M. J. BREVOORT

#### SUMMARY

*This investigation is part of an extensive experimental study that has been carried out at full scale in the N. A. C. A. 20-foot tunnel, the purpose of which has been to furnish information in regard to the functioning of the propeller-cowling-nacelle unit under all conditions of take-off, climbing, and normal flight. This report presents the results of tests of six propellers in the normal and high-speed flight range and also includes a study of the take-off characteristics. The range of the advance-diameter ratio has been extended far beyond that of earlier full-scale experiments at the Laboratory, blade-angle settings up to 45° being included, which are equivalent to air speeds of more than 300 miles per hour for propellers of normal size and revolution speed. All the propellers were tested in conjunction with a standard nacelle unit equipped with half a dozen representative N. A. C. A. cowlings.*

*The results show very striking differences in the aerodynamic qualities of the various propellers, particularly in the high-speed range. Also of interest is the fact that the conventional propeller is shown to reach its peak efficiency in a range of 200 to 350 miles per hour and at a blade angle of approximately 35°. The inadequacy of using the propulsive efficiency unconditionally as a figure of merit is shown. This efficiency, defined in conventional manner, is found actually to exceed unity in certain cases, owing to the fact that certain cowlings show a decreased drag in the propeller slipstream. The adoption of some standard nacelle unit is therefore recommended as a basis for the comparative testing of propellers. The experimental results are presented in convenient charts. Charts for practical use in selecting propeller diameters and charts for choosing the optimum blade-angle setting in the take-off range are given in an appendix.*

#### INTRODUCTION

The reported investigation is part of a comprehensive study of cowling-nacelle-propeller combinations (references 1 and 2). The tests were conducted in the N. A. C. A. 20-foot tunnel (reference 3) of full-size commercial propellers over the full range of blade angles up to 45° and over the full range of tunnel speeds up to

about 100 miles per hour. Recent rapid increase in the speed of airplanes has produced a need for tests extending to large values of the advance-diameter ratio  $V/nD$ . To the knowledge of the authors this is the first time that the effect of the cowling form on the propeller has been systematically investigated and that a series of full-scale propellers has been tested up to 45° blade angle.

It has been mentioned elsewhere (reference 1) that the quantity  $P_c = \frac{P}{qSV}$  (where  $P$  is the power supplied to the propeller shaft,  $S$  the disk area,  $V$  the velocity, and  $q$  the velocity head of the air stream) represents the contraction of the propeller slipstream. It will be referred to as the "unit disk loading" or "disk-loading coefficient."

The great convenience of using the quantity  $P_c$  in comparing the results of tests of various propellers is realized. The ideal efficiency is directly a function of  $P_c$ . For a given horsepower and propeller size,  $P_c$  is proportional to the inverse of the third power of the air speed. For this reason the various diagrams are based on  $1/\sqrt[3]{P_c}$  rather than on  $P_c$ , the abscissa thus being proportional to the air speed. The various efficiencies have in several cases been plotted against this quantity. For practical purposes of choosing propeller diameters for given values of the other variables, it is perfectly possible to include curves of constant  $V/nD$  and blade-angle setting. All practical values may, however, be obtained directly from the contour charts given in the appendix, which are based on the experimental results of this investigation.

Equal values of  $P_c$  actually correspond to similar flow conditions through the propeller disk and around the nacelle. A test to simulate a speed of 300 miles per hour may thus be run at 100 miles per hour tunnel speed with the value of  $P_c$  adjusted to give the identical slipstream contraction. This value is obtained by reducing the thrust to 1/9 or the power supplied to the shaft to 1/27 of the actual values at 300 miles per hour. The test is thus actually conducted at a scale or Reynolds Number of 1/3 of the full-scale values. Experience shows, however, that no particular Reynolds Number

effect is expected in this range since the tests are conducted far beyond the usual model range. On the other hand, the reported tests were all conducted at tip speeds far below sound velocity and the results may

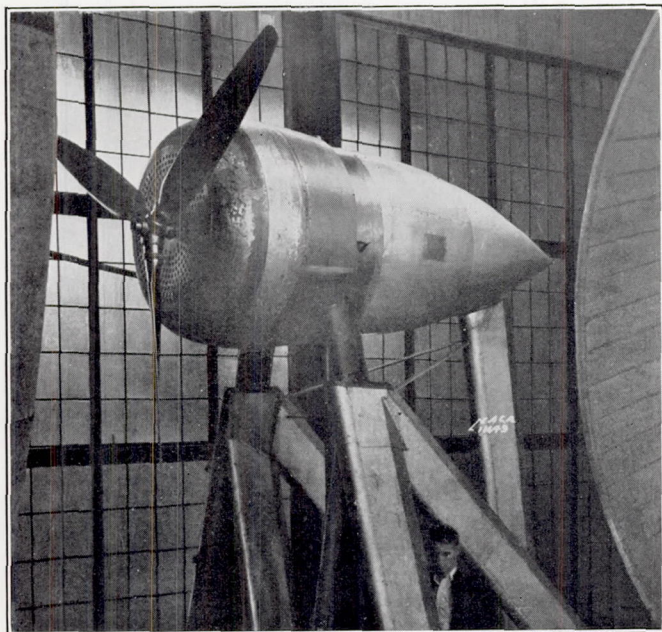


FIGURE 1.—Test model with nose 18 and propeller B mounted on the balance frame in the 20-foot wind tunnel.

be considered free from any effects of the compressibility of the air.

As will be evident from the test results, the propulsive efficiency alone as defined in the usual manner is not a dependable criterion of the efficiency of the propeller tested in conjunction with a nacelle but is quite dependent on the particular nacelle or body used behind the propeller. This efficiency is therefore significant only if the various propellers are tested on the identical nacelle. For this reason a quantity termed the "net efficiency," which relates to the entire propeller-nacelle unit, has been used throughout this report. It is defined as

$$\eta_n = \frac{RV}{P}$$

where  $R$  is the net forward thrust of the entire unit as measured on the thrust scale. This quantity is in itself a perfectly arbitrary reference number, depend-

ing largely on the relative dimensions of the propeller and the nacelle.

Since the same nacelle has been used throughout the entire test series, it is certain that the combination giving the highest net efficiency under any specified condition is superior to any other combination. The net efficiency may be considered as containing the propulsive efficiency together with the efficiency of the cowling-nacelle.

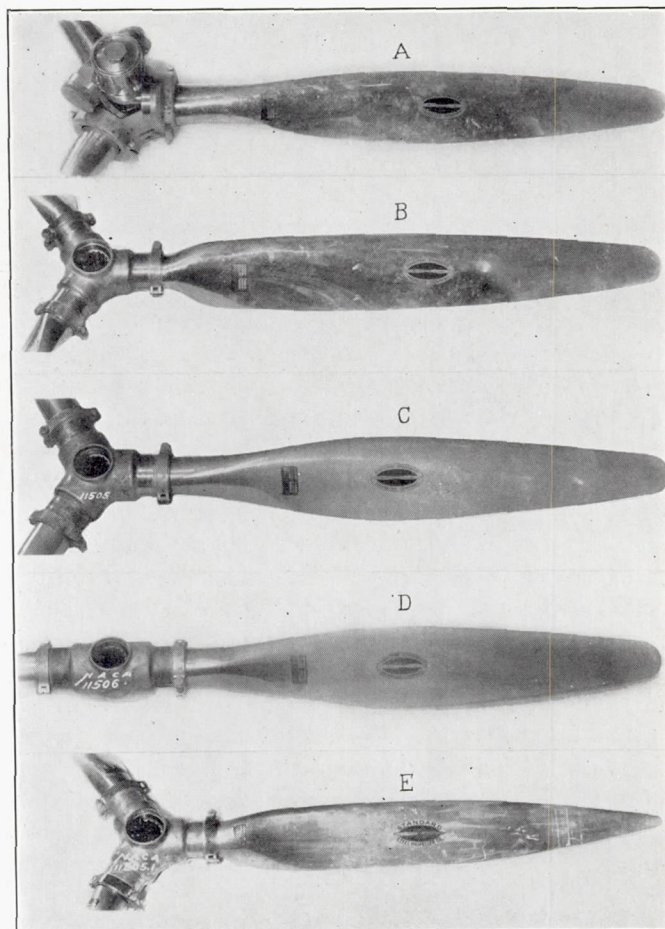


FIGURE 2.—Propellers used in the investigation.

#### DESCRIPTION OF TESTS

Figure 1 is a photograph of the installation in the 20-foot tunnel used for this investigation. Figure 2 shows the propellers used, the complete details of which are shown in figure 3 and in the following table.

#### PROPELLERS

Propeller designation	Drawing	Number of blades	Diameter	Type	Remarks	Airfoil section
A	Hamilton Standard 6101-0.....	3	Feet 10.06	Controllable.....	.....	Clark Y.
B	Hamilton-Standard 1C1-0.....	3	10.04	Adjustable.....	Blade section same as A except near hub.....	Do.
B <sub>x</sub>	Hamilton-Standard 1C1-0 (modified).....	3	10.04	do.....	Blade angle decreased from the 70-percent radius to the tip (fig. 3).	Do.
C	Navy plan form 5868-9.....	3	10.02	do.....	.....	Do.
D	Navy plan form 5868-9.....	2	10.00	do.....	Same as C except 2 blades.....	Do.
E	Navy plan form 3790.....	3	9.04	do.....	.....	R. A. F.-6.

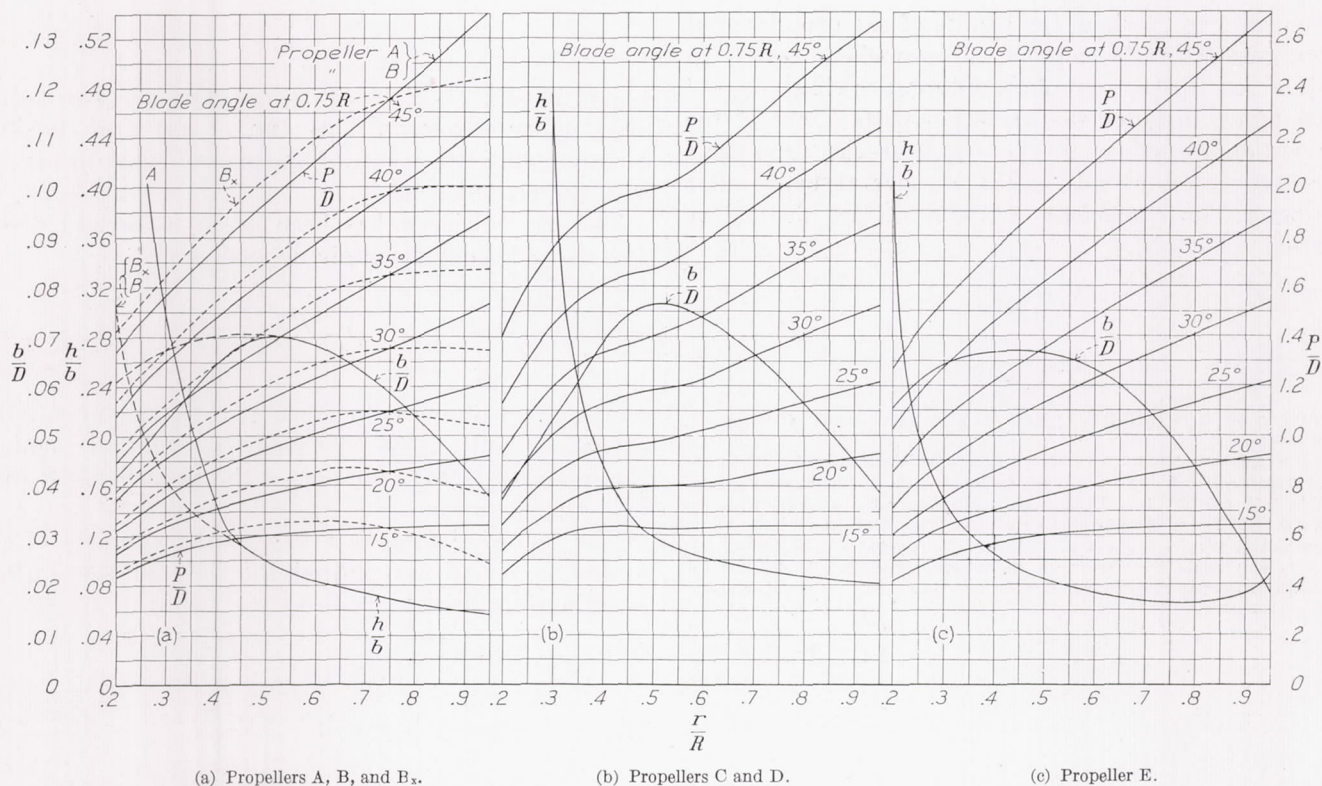


FIGURE 3.—Blade-form curves for the propellers tested.  $D$ , diameter;  $b$ , blade width;  $h$ , blade thickness;  $P$ , pitch;  $R=D/2$ , radius at tip;  $r$ , radius.

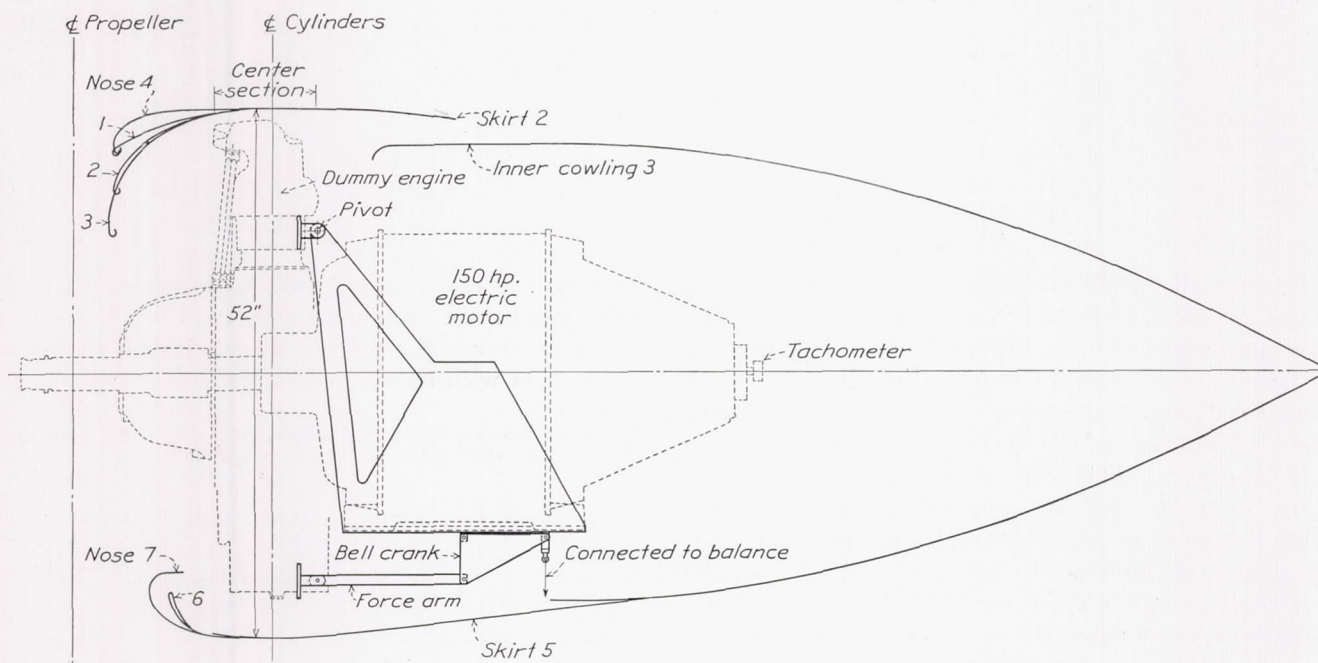


FIGURE 4.—Test arrangement and cowling shapes used in the propeller investigation.

The drawing in figure 4 shows in detail the nacelle unit with the particular noses and skirts used in the propeller tests. Power to the propeller was furnished by a variable-speed electric motor en-

closed in the nacelle unit. The propellers were tested up to and including a blade angle of  $45^\circ$  at  $0.75R$  and at tunnel speeds up to more than 100 miles per hour.



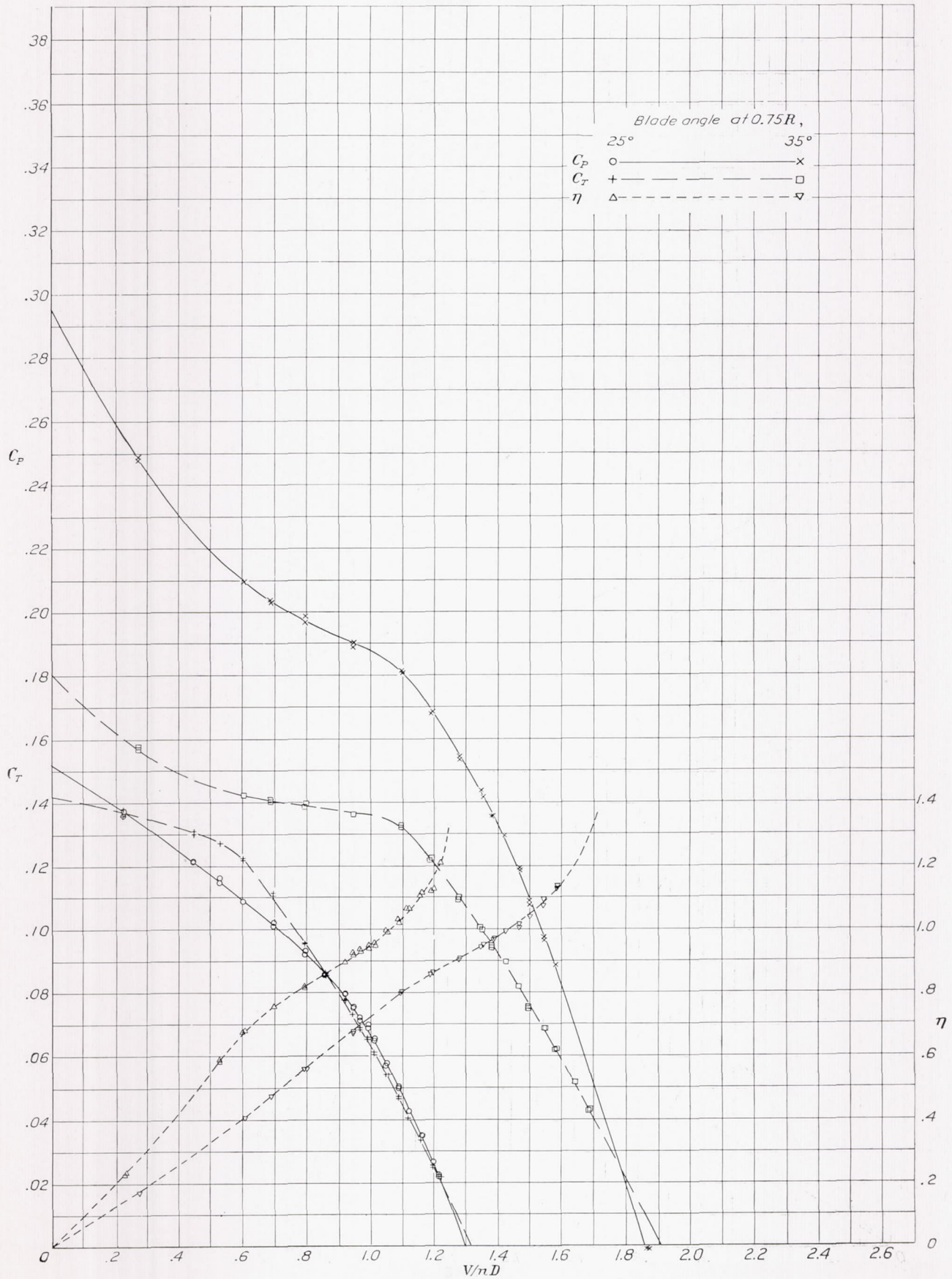


FIGURE 5.—Curves of  $C_T$ ,  $C_P$ , and  $\eta$  against  $V/nD$  for nose 1, propeller B.

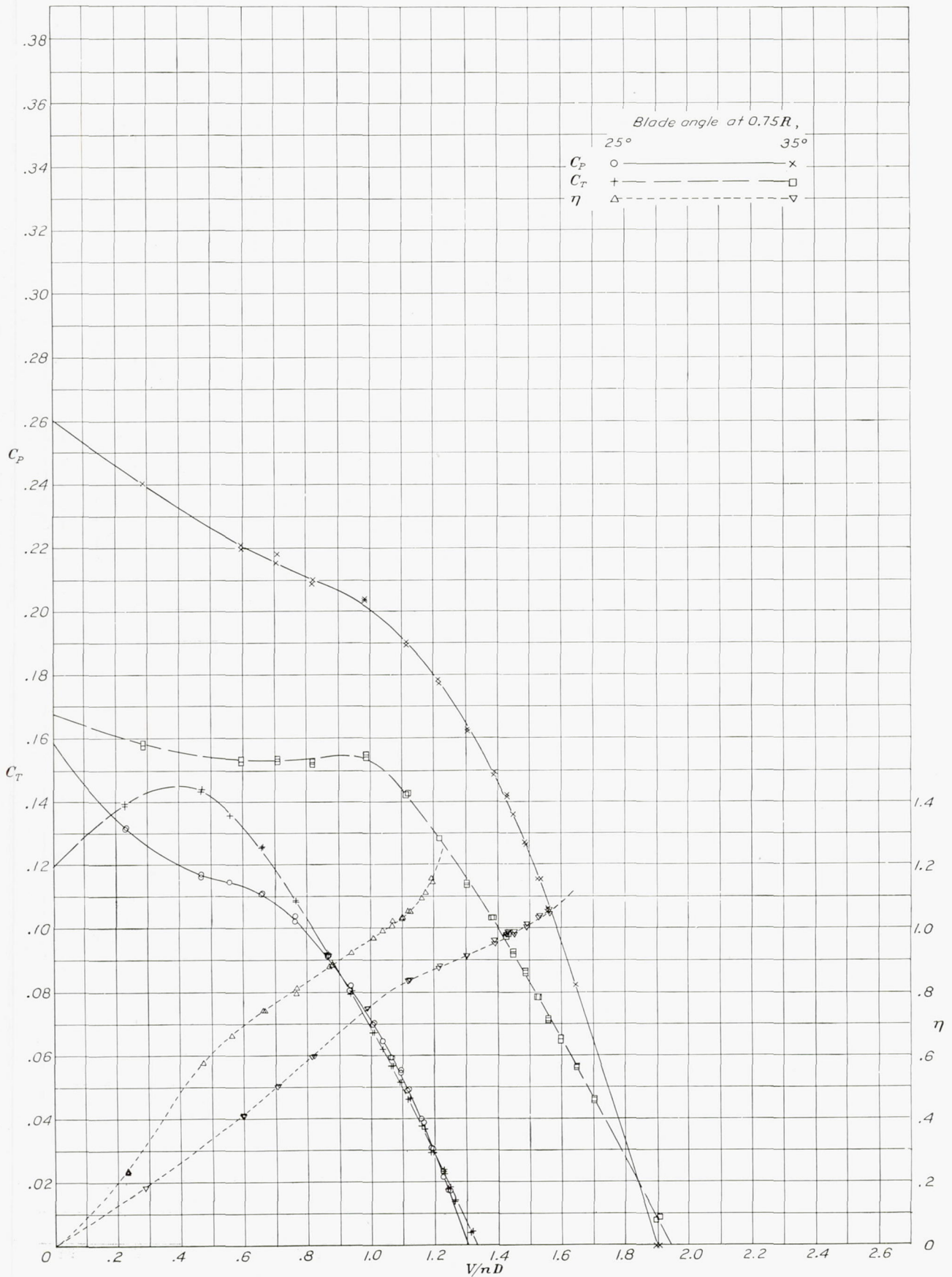


FIGURE 6.—Curves of  $C_T$ ,  $C_P$ , and  $\eta$  against  $V/nD$  for nose 1, propeller C.

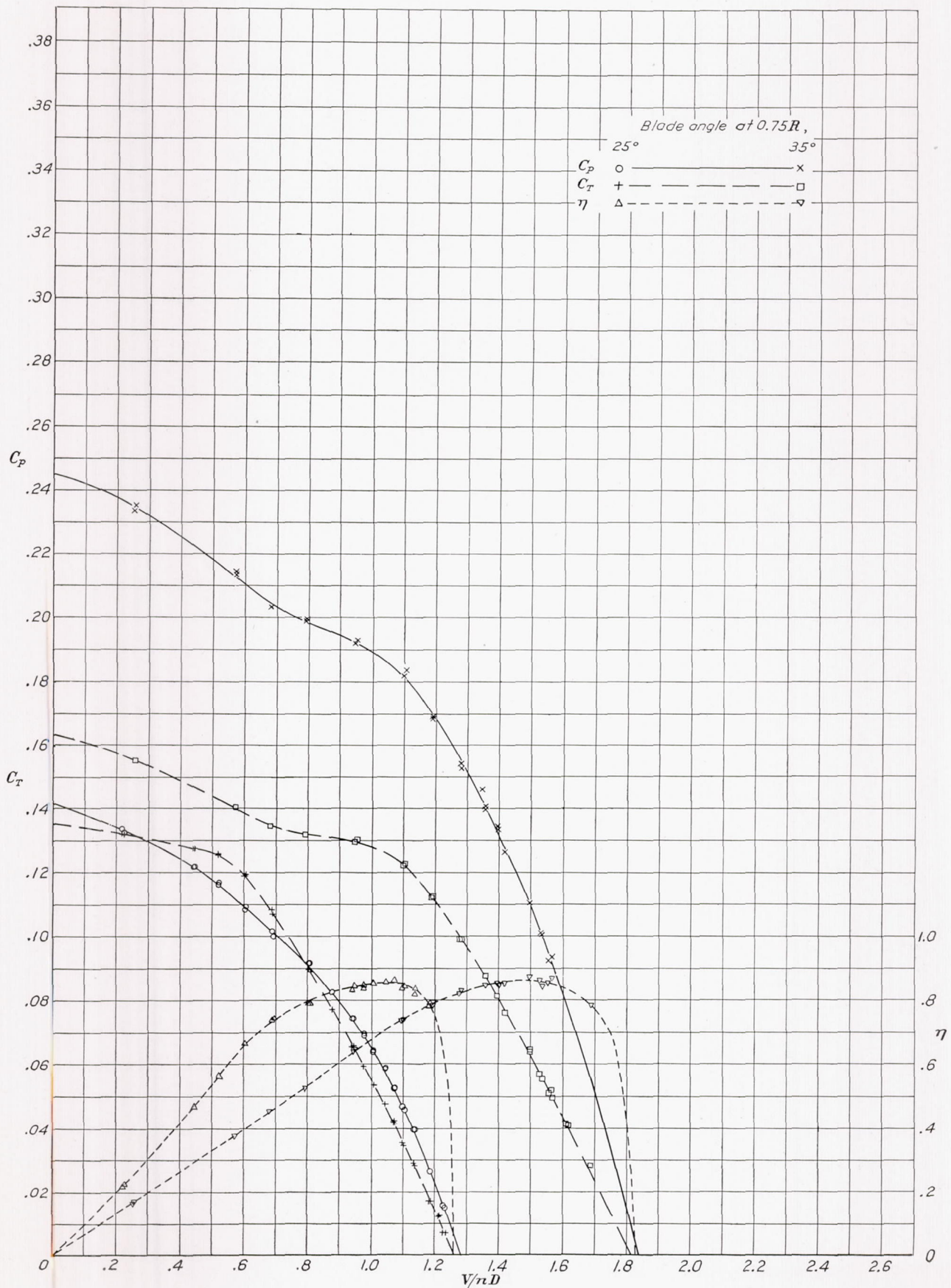


FIGURE 7.—Curves of  $C_T$ ,  $C_p$ , and  $\eta$  against  $V/nD$  for nose 2, propeller B.

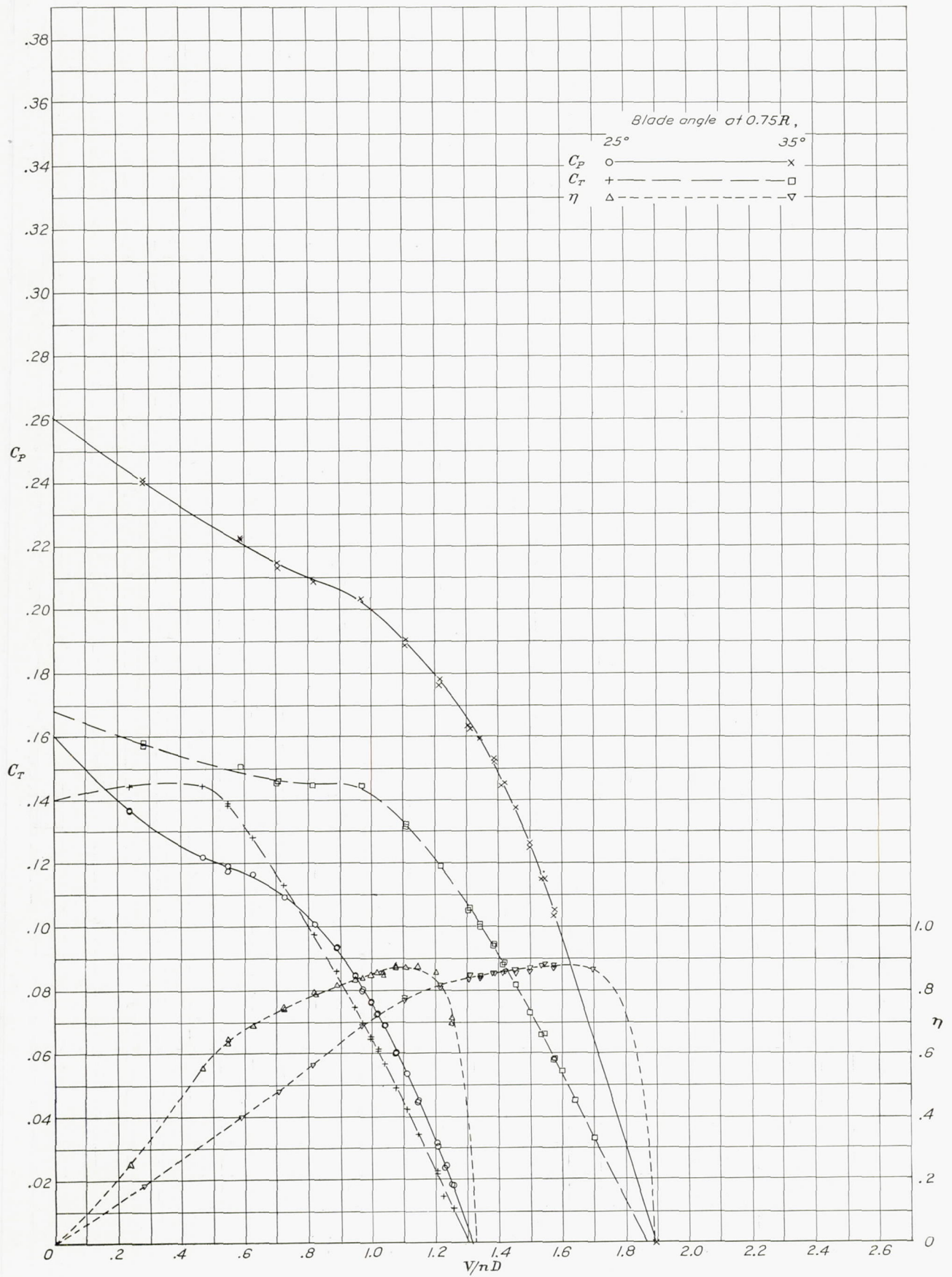


FIGURE 8.—Curves of  $C_T$ ,  $C_p$ , and  $\eta$  against  $V/nD$  for nose 2, propeller C.

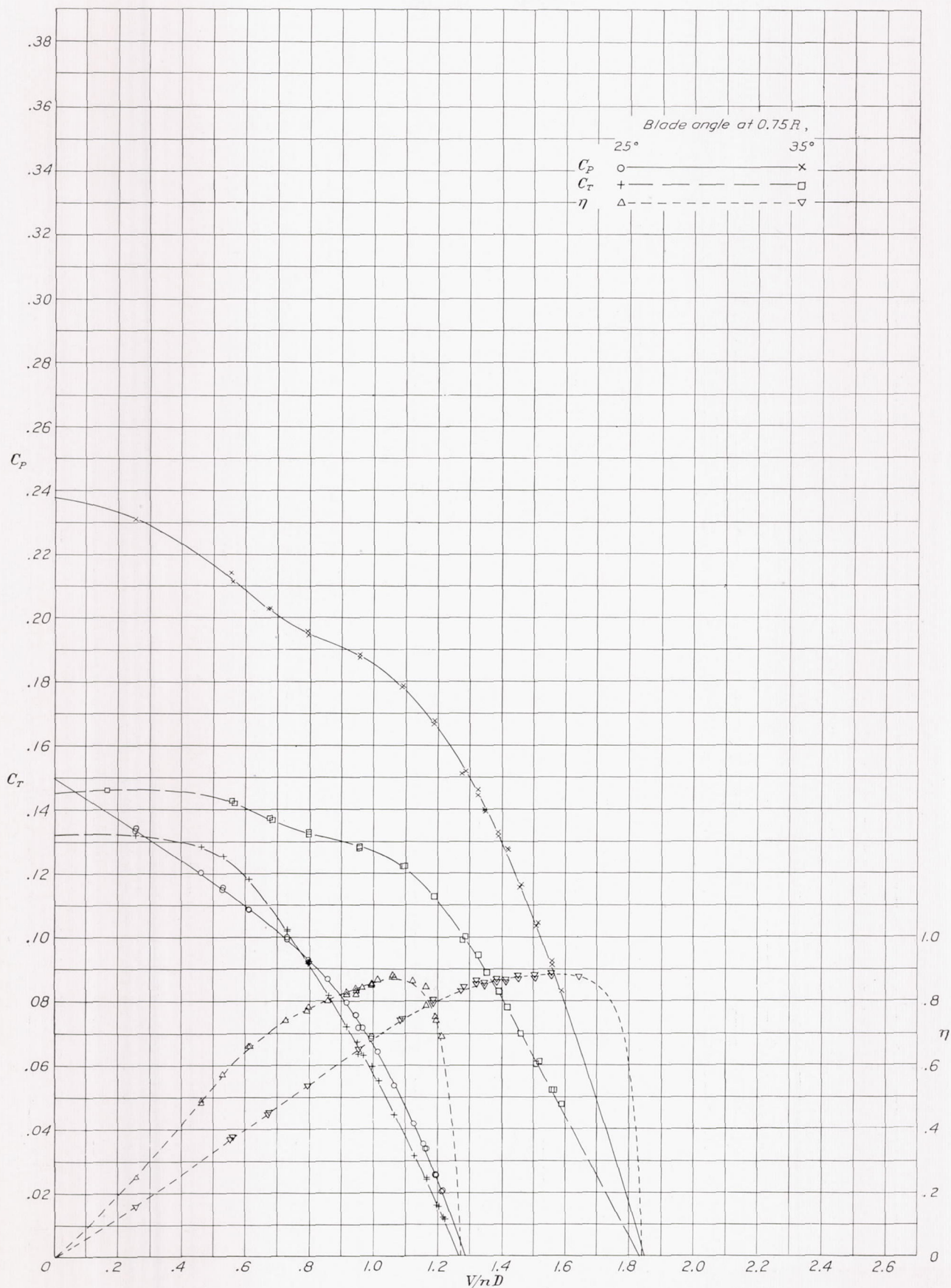


FIGURE 9.—Curves of  $C_T$ ,  $C_P$ , and  $\eta$  against  $V/nD$  for nose 3, propeller B.

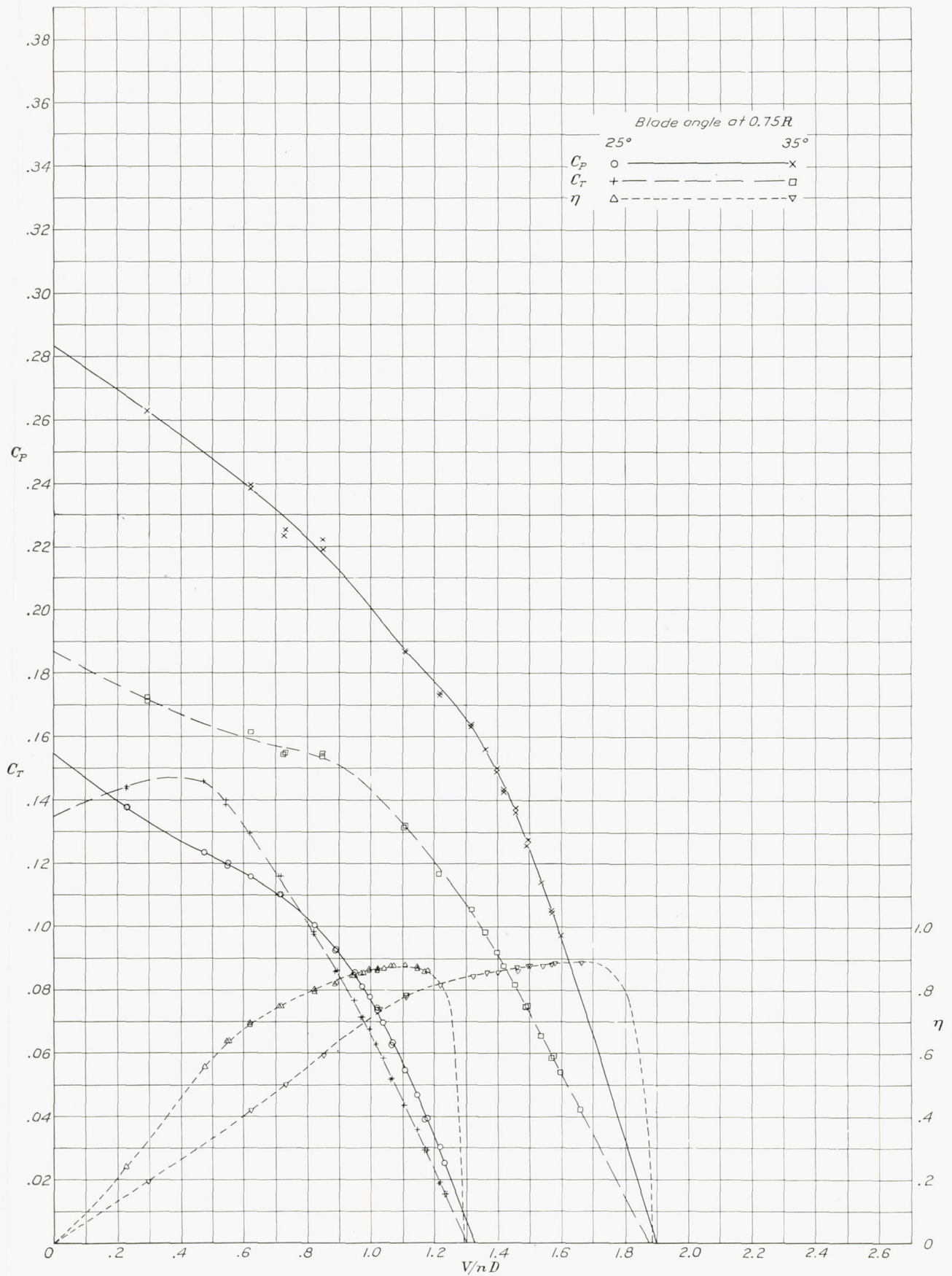


FIGURE 10.—Curves of  $C_T$ ,  $C_P$ , and  $\eta$  against  $V/nD$  for nose 3, propeller C.

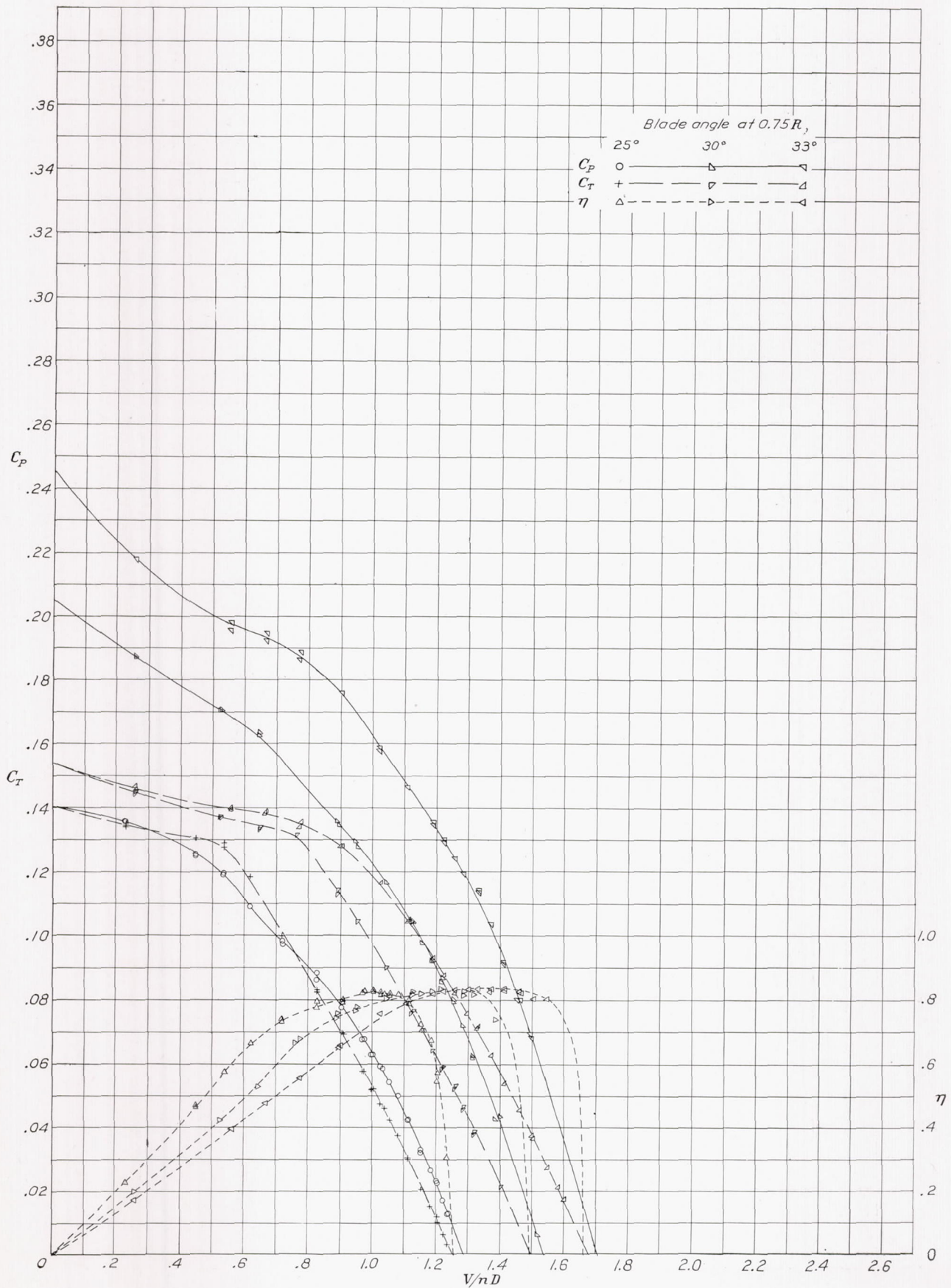


FIGURE 11.—Curves of  $C_T$ ,  $C_p$ , and  $\eta$  against  $V/nD$  for nose 4, propeller B.

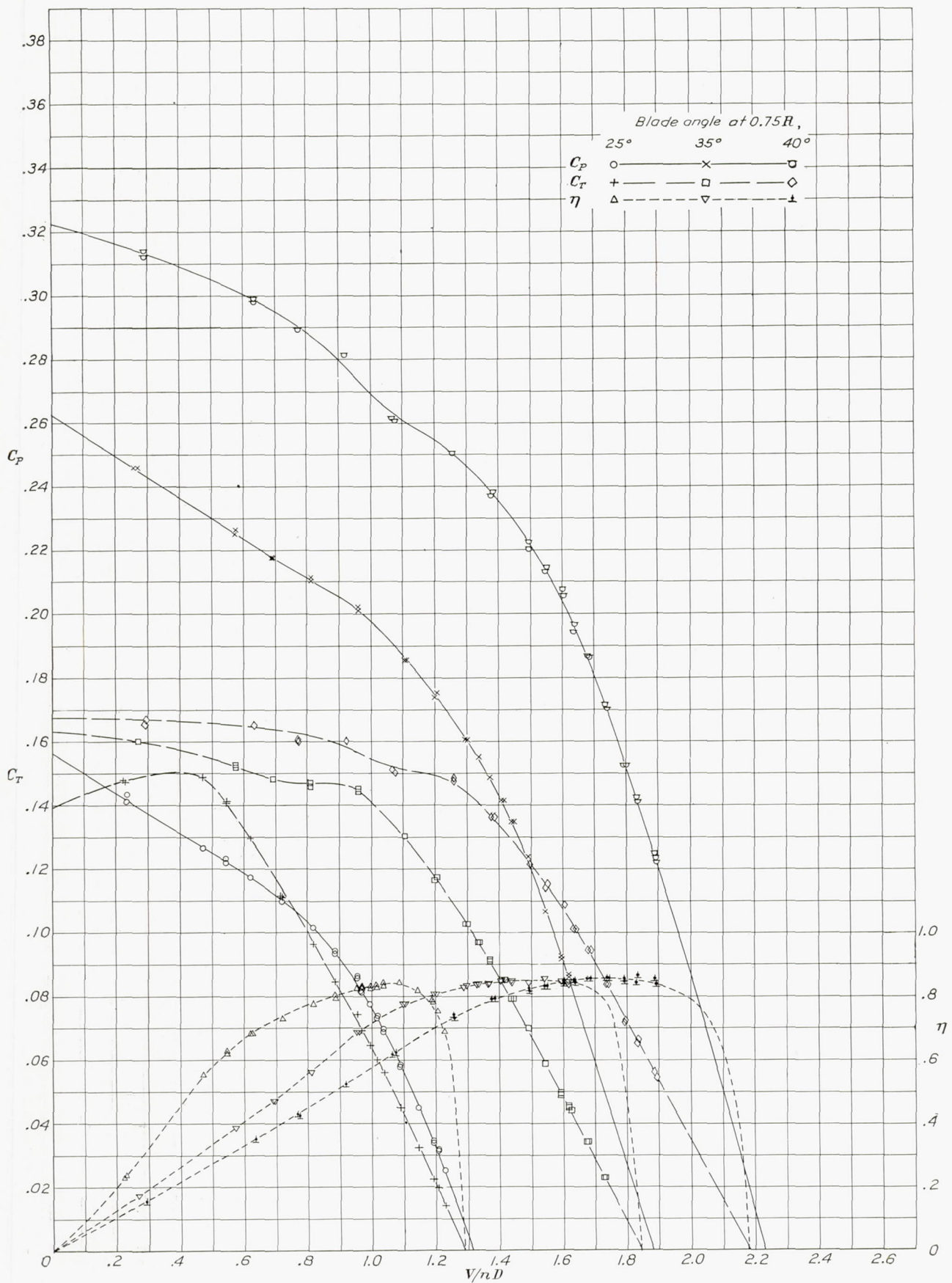


FIGURE 12.—Curves of  $C_T$ ,  $C_p$ , and  $\eta$  against  $V/nD$  for nose 4, propeller C.

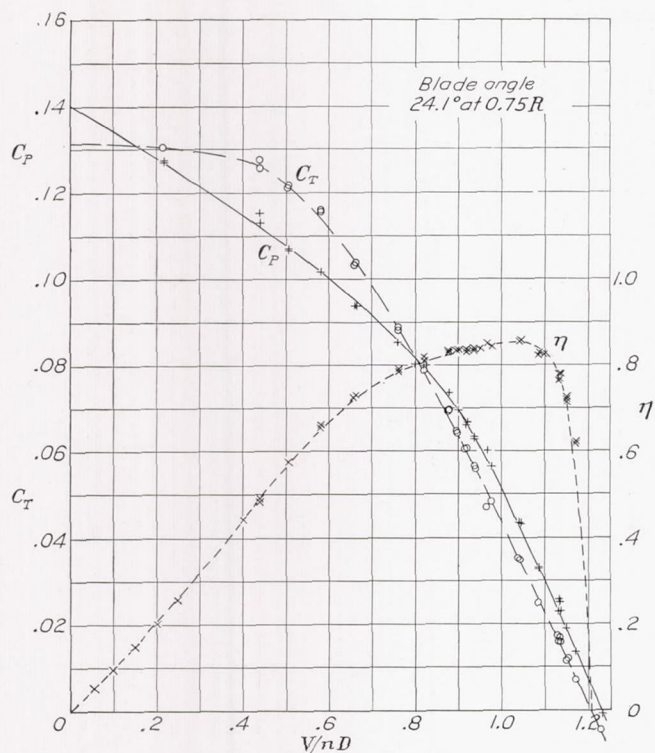


FIGURE 13.—Curves of  $C_T$ ,  $C_P$ , and  $\eta$  against  $V/nD$  for nose 4, propeller A.

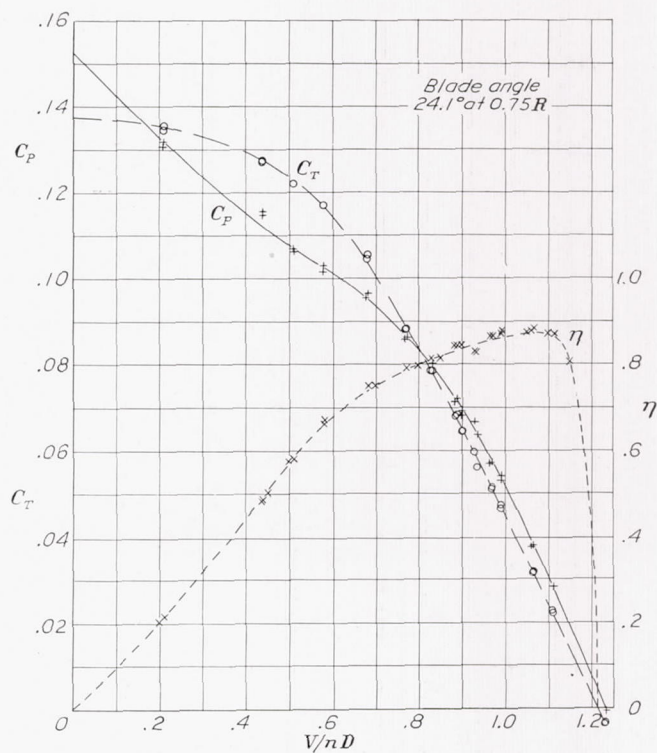


FIGURE 14.—Curves of  $C_T$ ,  $C_P$ , and  $\eta$  against  $V/nD$  for nose 6, propeller A.

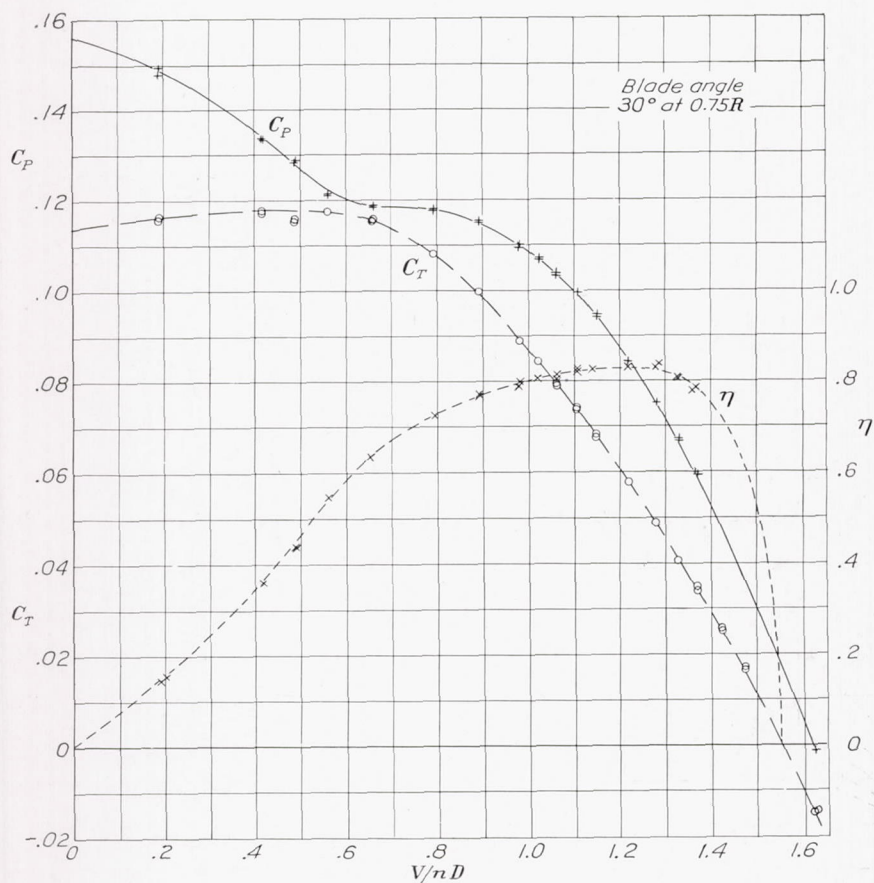


FIGURE 15.—Curves of  $C_T$ ,  $C_P$ , and  $\eta$  against  $V/nD$  for nose 4, propeller E.

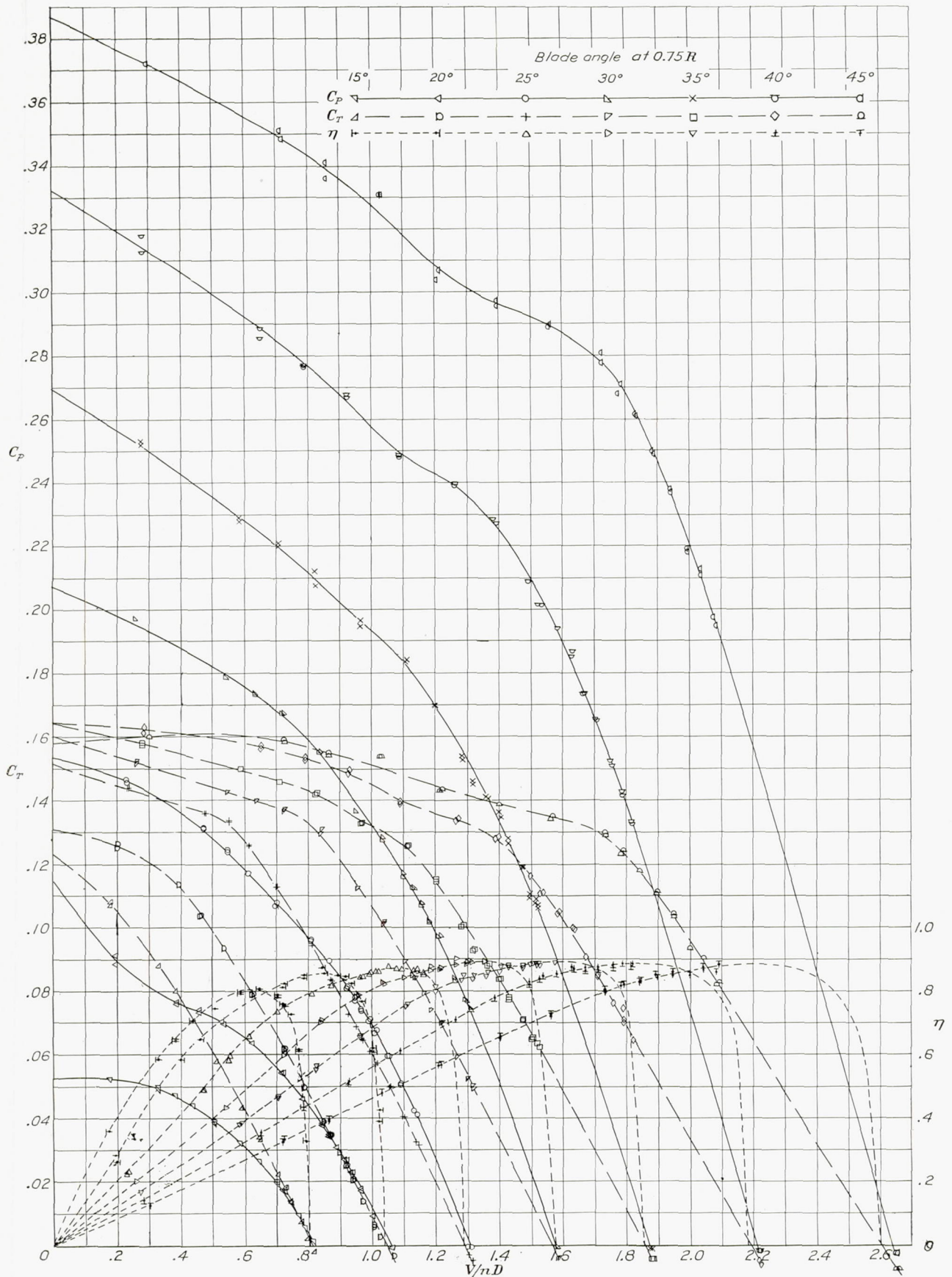


FIGURE 16.—Curves of  $C_T$ ,  $C_p$ , and  $\eta$  against  $V/nD$  for nose 6, propeller B.

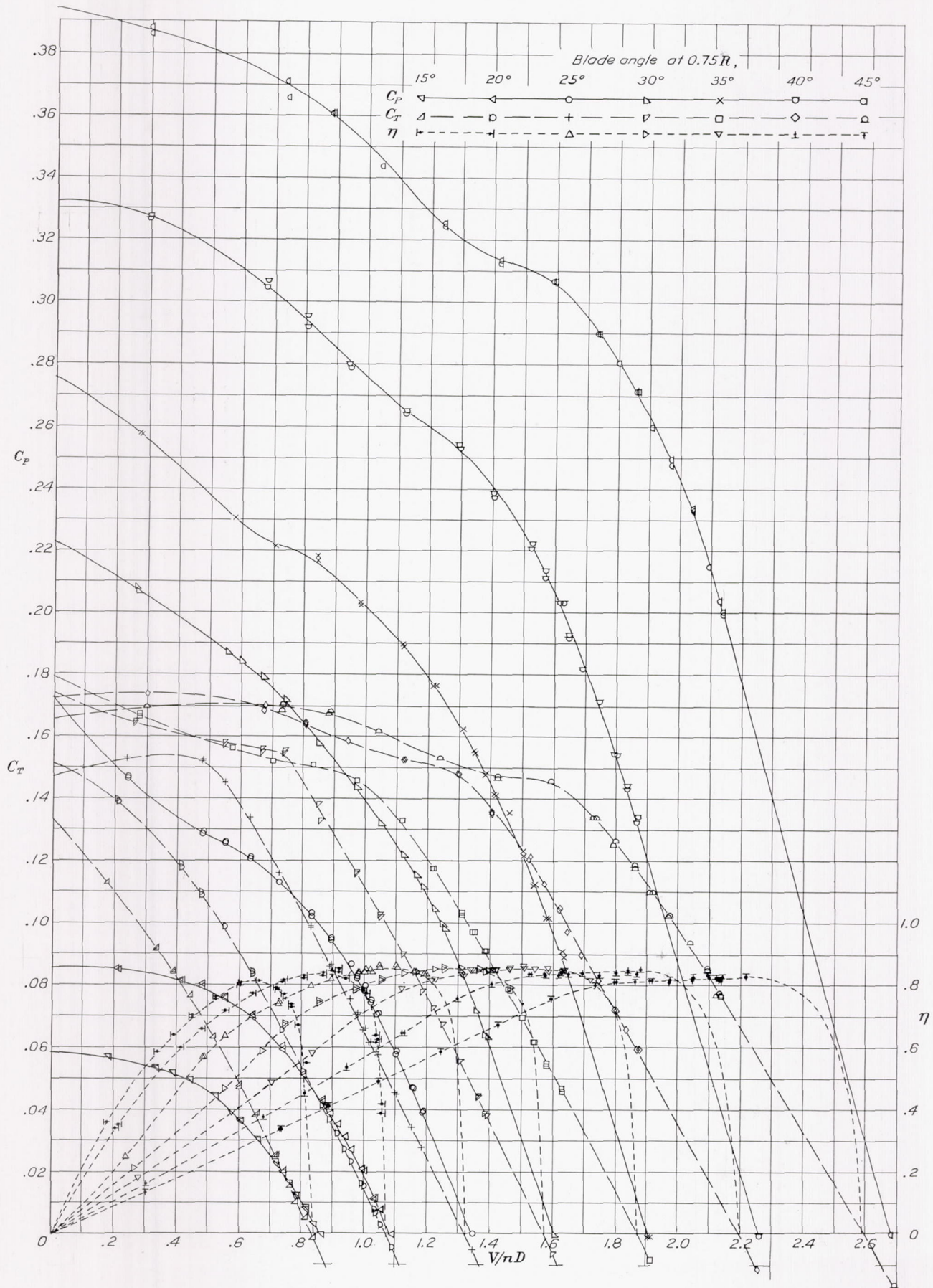


FIGURE 17.—Curves of  $C_t$ ,  $C_p$ , and  $\eta$  against  $V/nD$  for nose 6, propeller C.

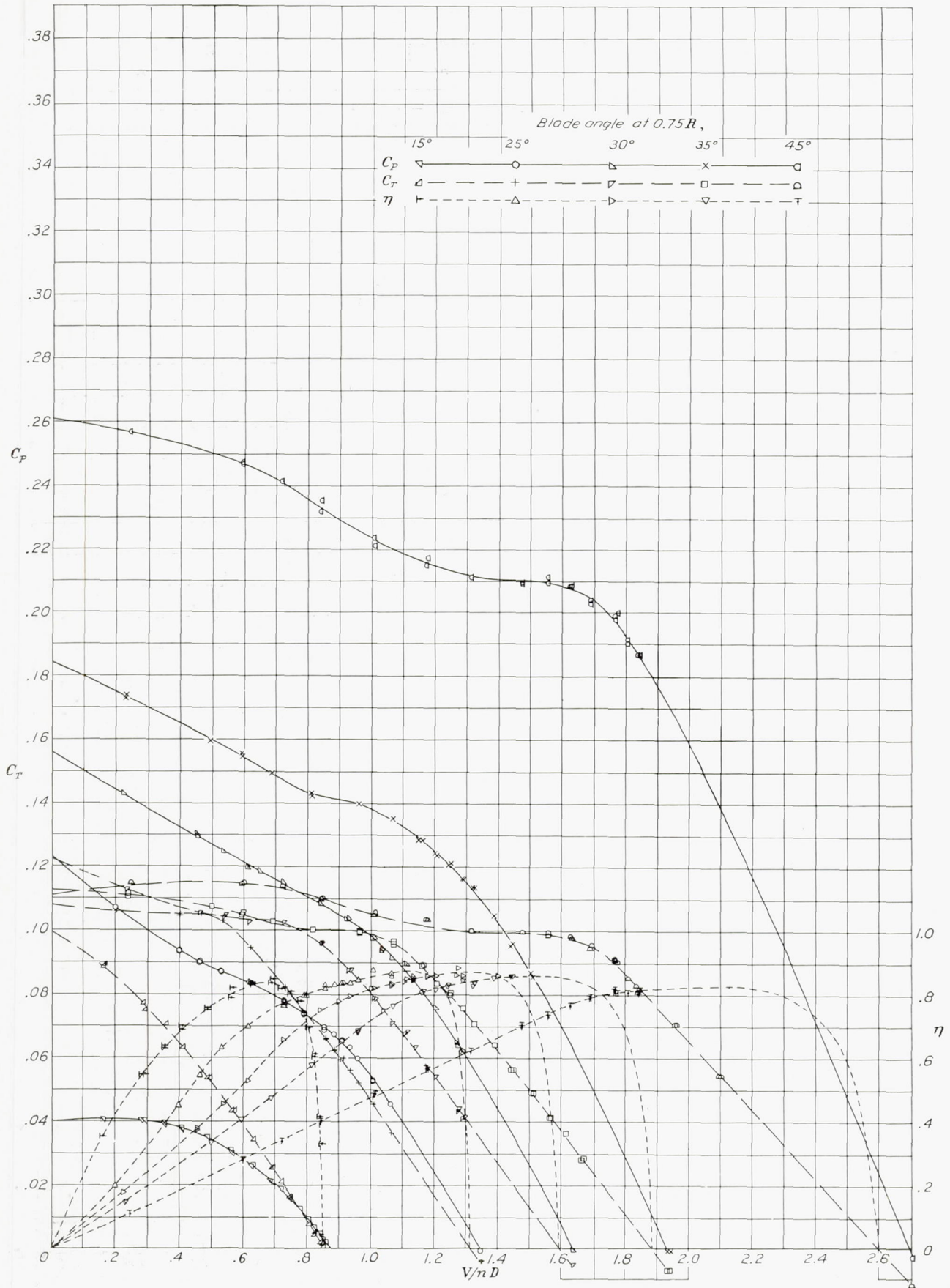


FIGURE 18.—Curves of  $C_T$ ,  $C_P$ , and  $\eta$  against  $V/nD$  for nose 6 propeller D.

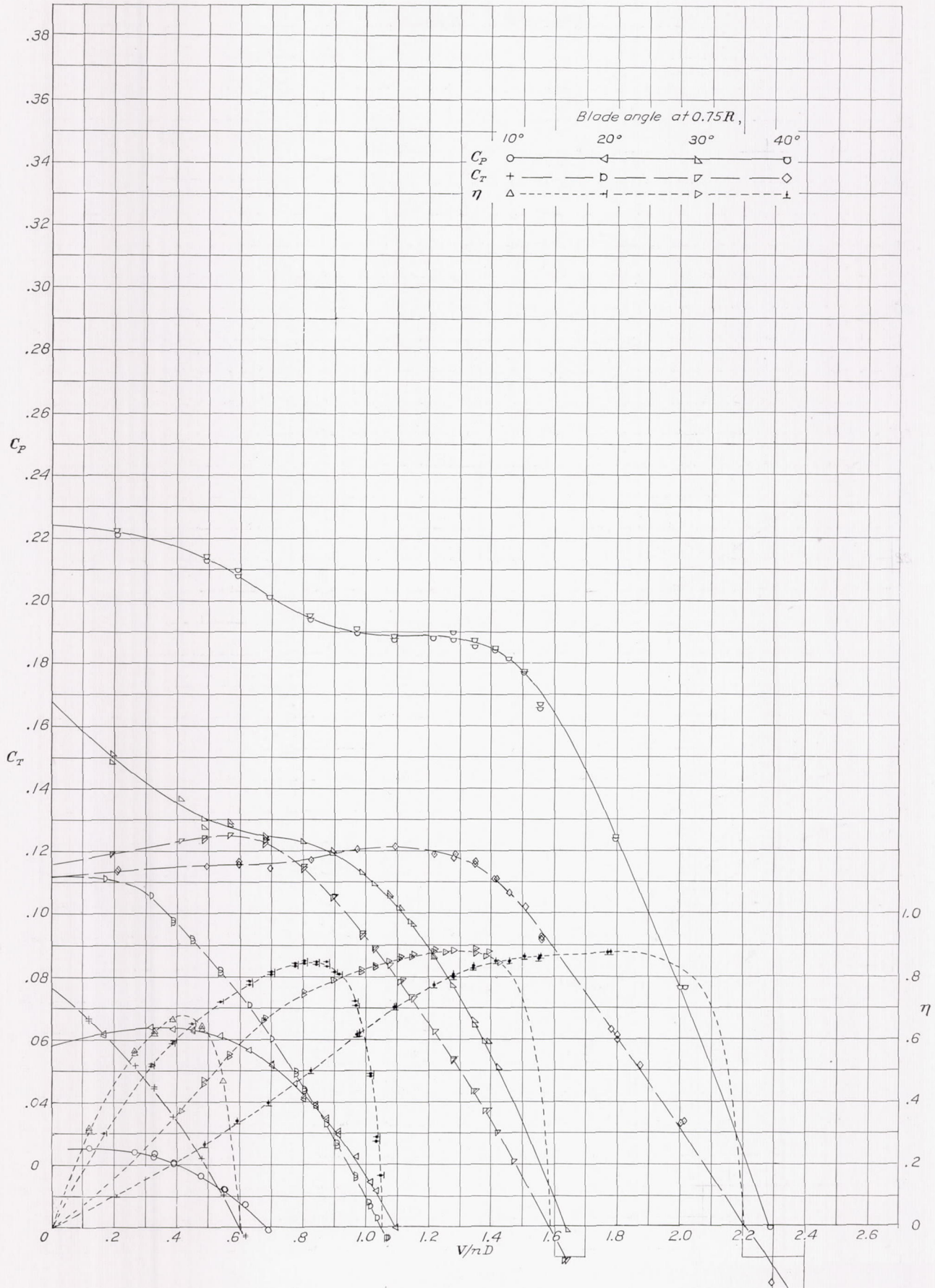


FIGURE 19.—Curves of  $C_T$ ,  $C_P$ , and  $\eta$  against  $V/\pi D$  for nose 6, propeller E.

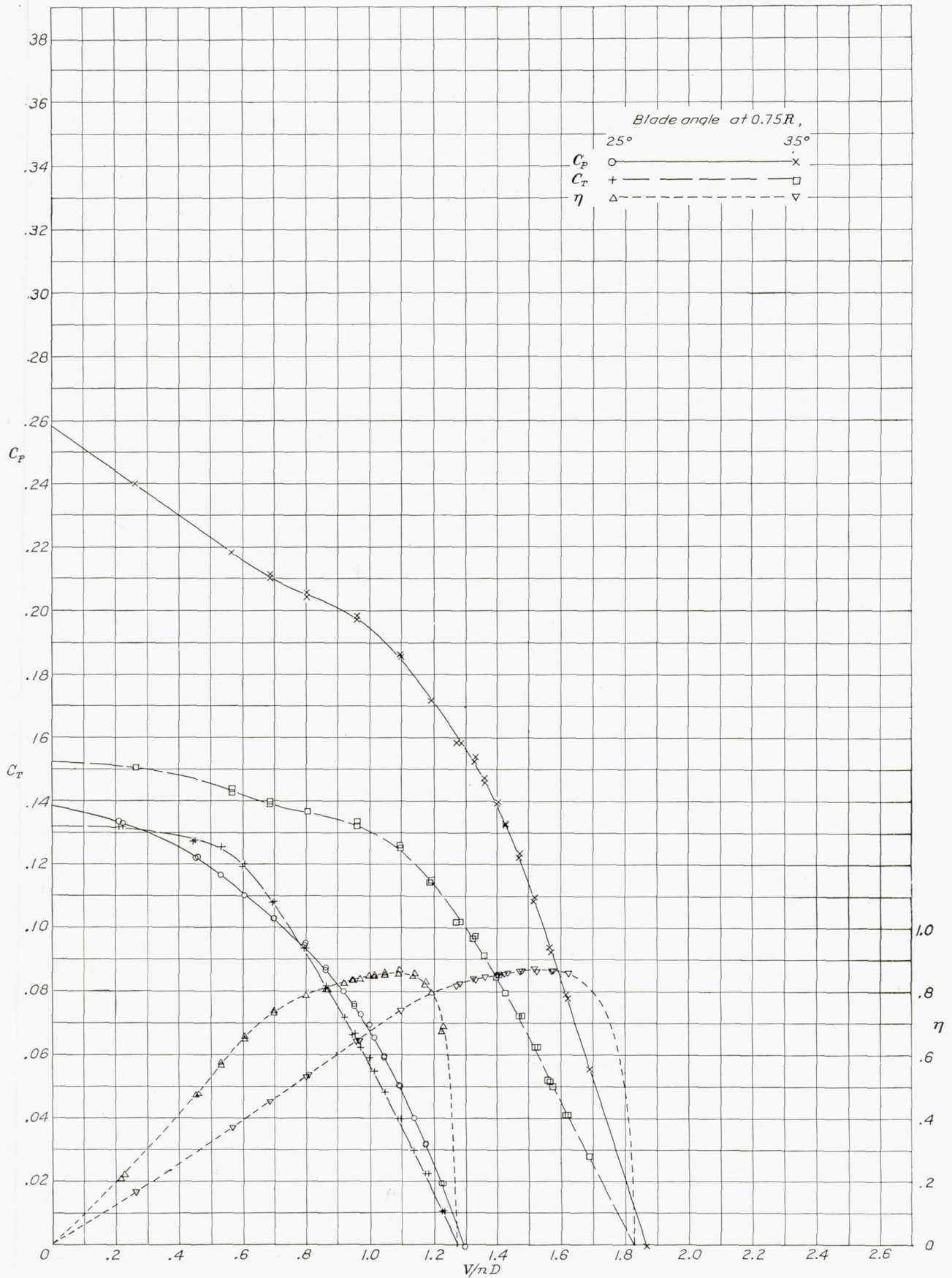


FIGURE 20.—Curves of  $C_T$ ,  $C_P$ , and  $\eta$  against  $V/nD$  for nose 7, propeller B.

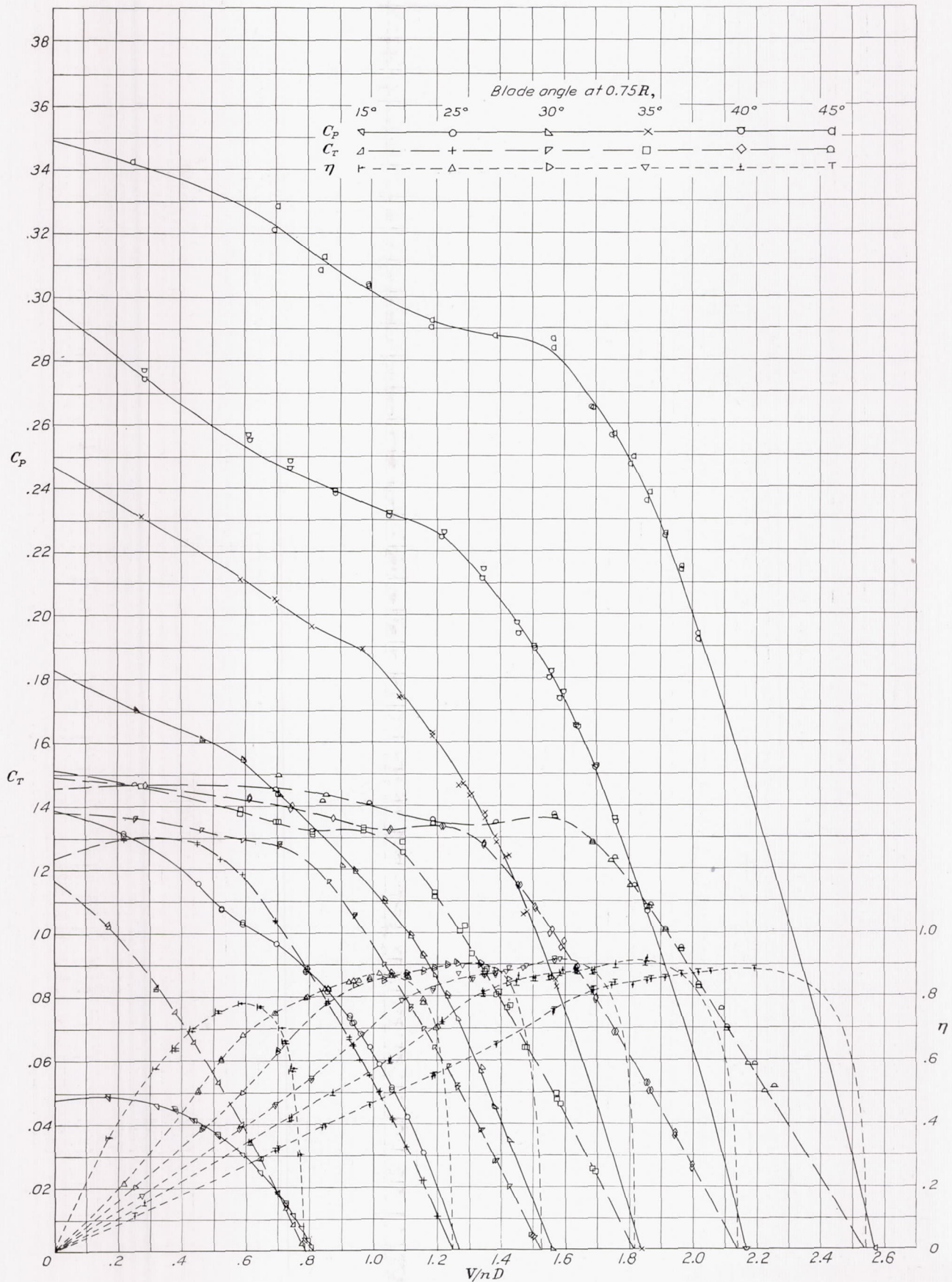


FIGURE 21.—Curves of  $C_T$ ,  $C_P$ , and  $\eta$  against  $V/nD$  for nose 7, propeller B<sub>x</sub>.

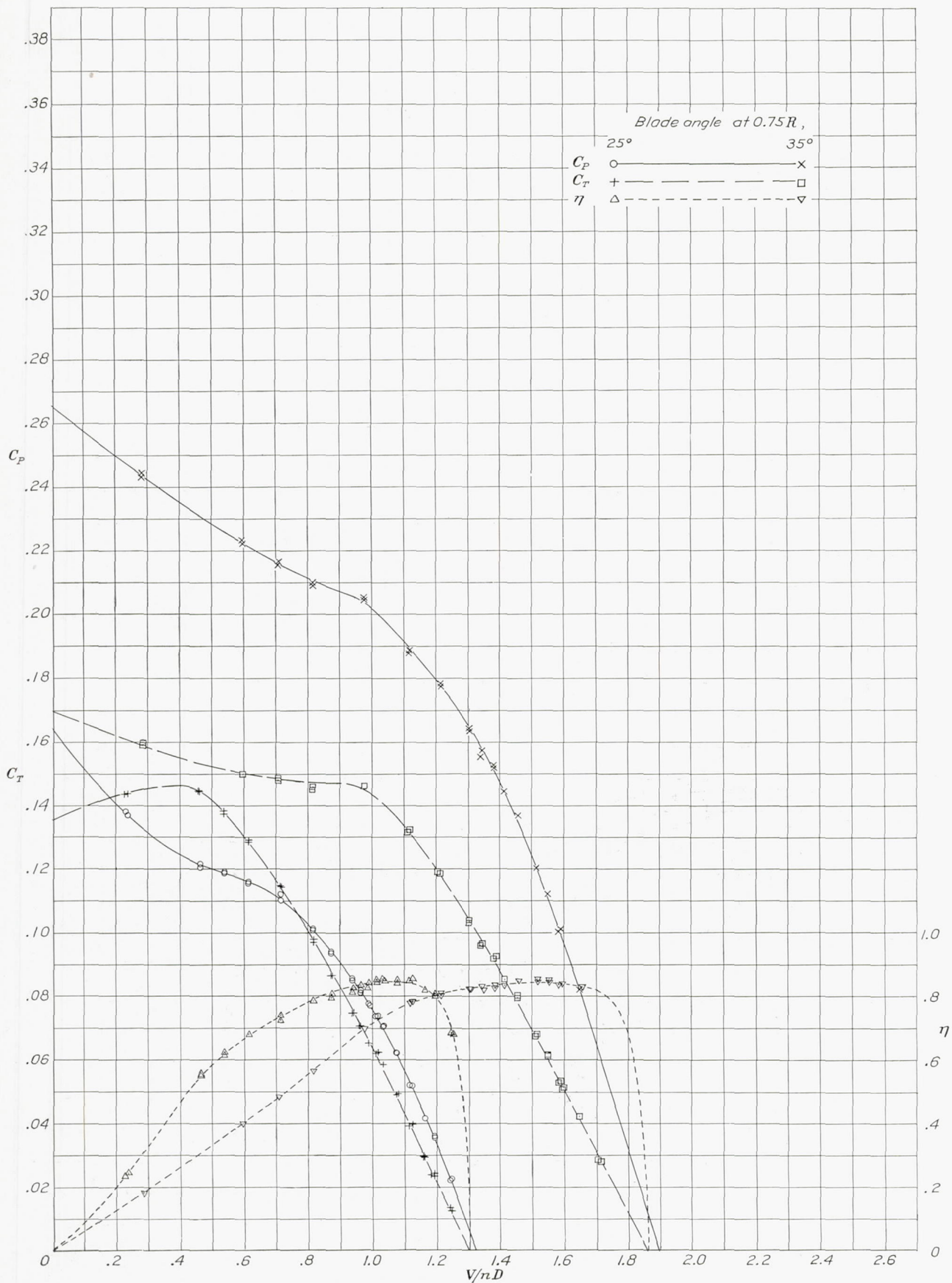


FIGURE 22.—Curves of  $C_T$ ,  $C_P$ , and  $\eta$  against  $V/nD$  for nose 7, propeller C.

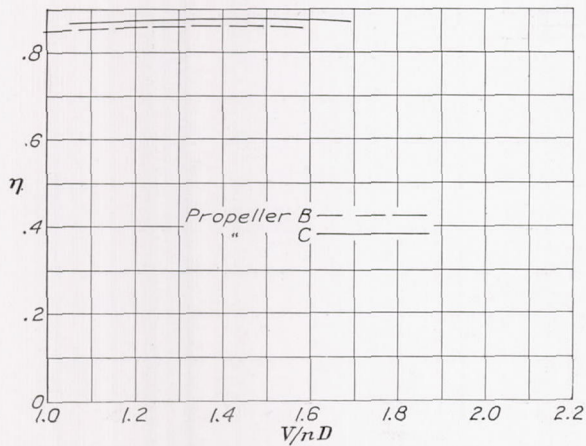


FIGURE 23.—Propulsive-efficiency envelopes against  $V/nD$  for propellers B and C on nose 2.

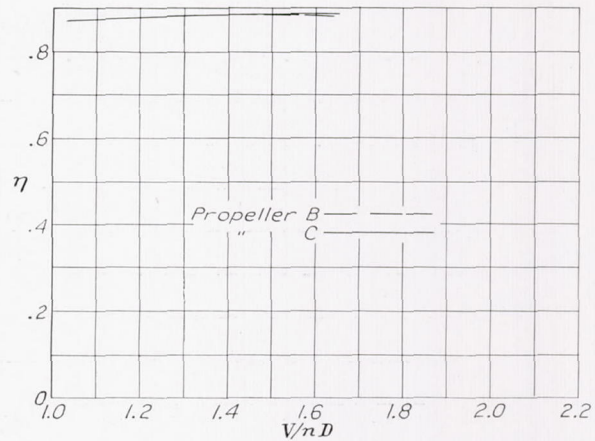


FIGURE 24.—Propulsive-efficiency envelopes against  $V/nD$  for propellers B and C on nose 3.

DISCUSSION OF RESULTS

It should be noticed that the propulsive efficiency in figure 5 is greater than 100 percent. The high value of this efficiency is caused by a certain peculiarity in the characteristics of nose 1, which has been pointed out in an earlier report (reference 1). It was shown in reference 1 that the drag of this particular nose decreased substantially with an increase in slipstream velocity owing to the fact that the local angle of attack at the leading edge of the cowling was sufficiently decreased to prevent a marked breakdown that occurred with the propeller off. This effect, which is quite contrary to the expectations of the theory, renders the practical use of the propulsive efficiency rather questionable. In other words, whenever some critical flow conditions exist that may be favorably affected by the propeller slipstream, it is perfectly possible to obtain efficiencies close to or in excess of unity. High efficiencies reported from time to time may easily be explained on this basis. There are, therefore, only two alternatives. One is to adopt a standardized cowling-

nacelle shape. Nose 7, described in reference 1, is particularly recommended for this purpose as being unusually neutral to the local flow condition at the nose. The other alternative is to avoid the use of the propulsive efficiency altogether by adopting some other figure of merit relating to the entire cowling-nacelle-

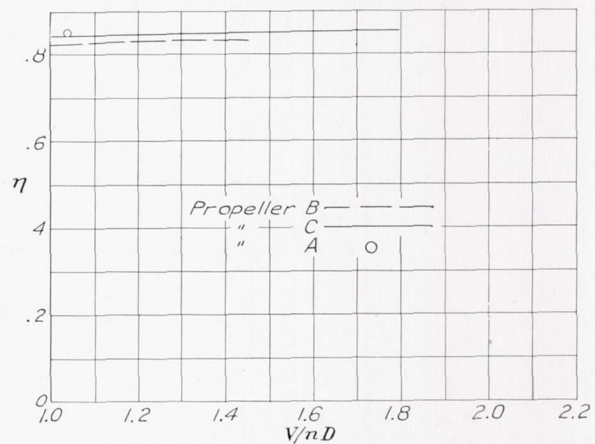


FIGURE 25.—Propulsive-efficiency envelopes against  $V/nD$  for propellers A, B, and C on nose 4.

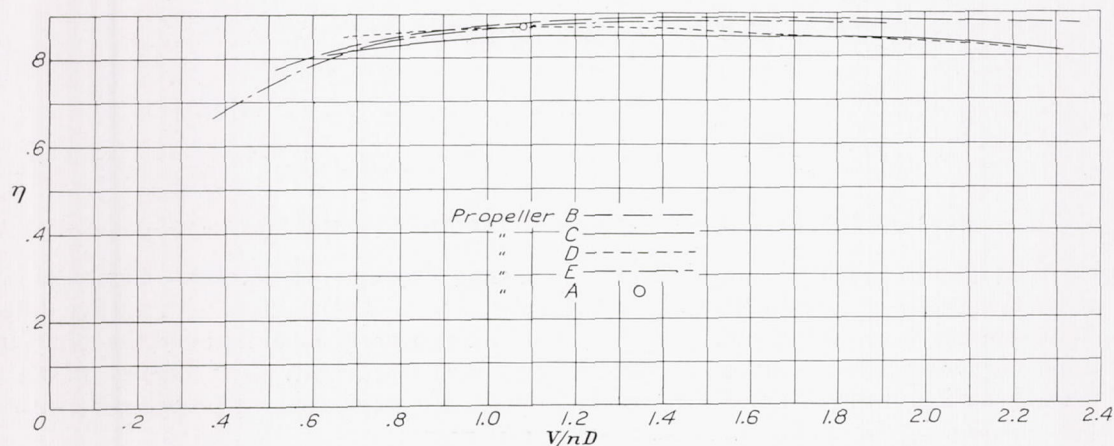
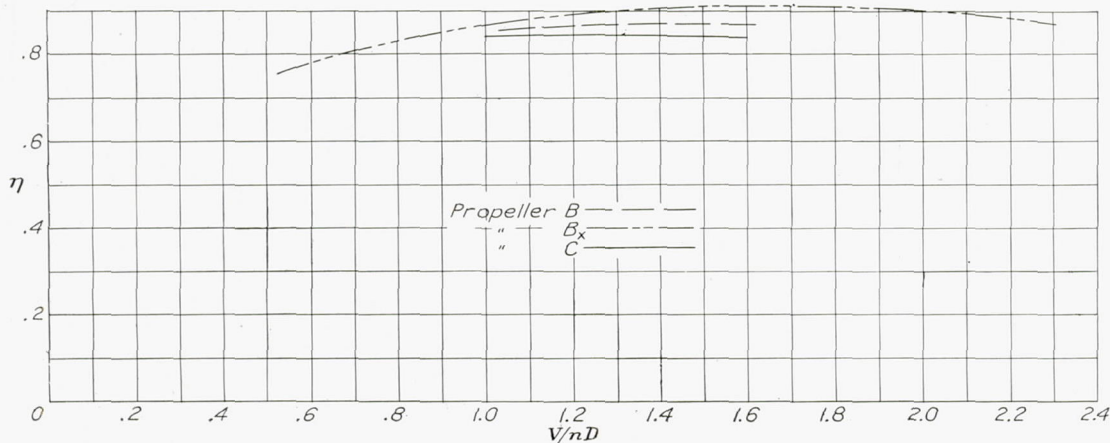
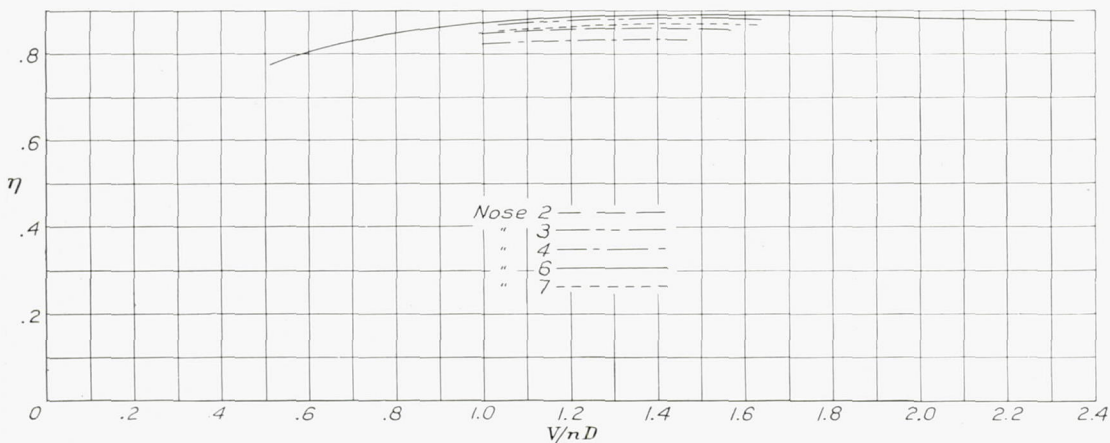
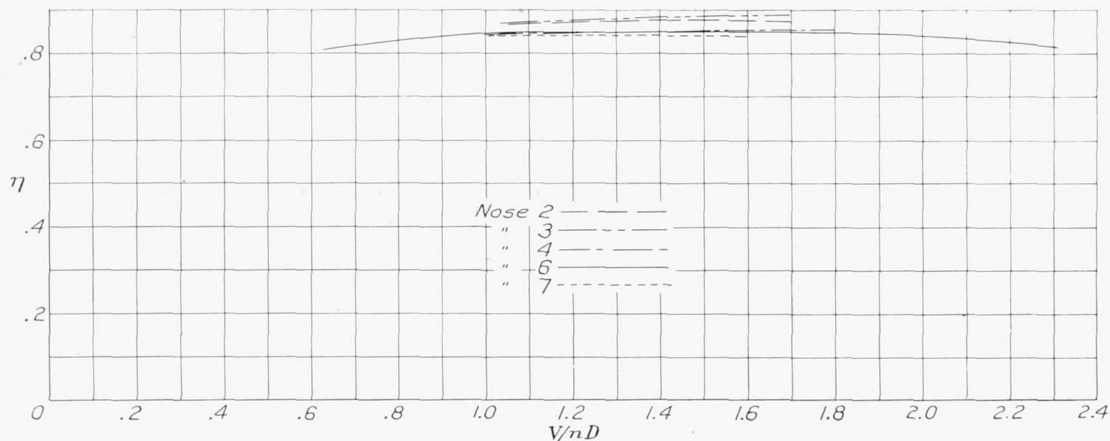


FIGURE 26.—Propulsive-efficiency envelopes against  $V/nD$  for propellers A, B, C, D, E on nose 6.

FIGURE 27.—Propulsive-efficiency envelopes against  $V/nD$  for propellers B,  $B_x$ , and C on nose 7.FIGURE 28.—Propulsive-efficiency envelopes against  $V/nD$  for noses 2, 3, 4, 6, and 7 with propeller B.FIGURE 29.—Propulsive-efficiency envelopes against  $V/nD$  for noses 2, 3, 4, 6, and 7 with propeller C.

propeller unit. The quantity defined as net efficiency has been used for this purpose. In the present report both these characteristics have been given.

The propulsive efficiencies given in figures 26 and 27 for the most neutral cowlings 6 and 7 show that propeller  $B_x$  is definitely superior to the others, exceeding the least efficient propeller by 4 to 6 percent. Figure 28 shows the results for propeller B in conjunction with five different cowlings. It will be seen that cowling 6 is superior, exceeding cowling 3 by 1 percent and

cowling 7 by about 2 percent. Figure 29 gives the results of tests of propeller C with the five different noses. In this case noses 3 and 2 exceed the others in efficiency by about 5 percent. The highest of all efficiencies obtained is 91 percent for propeller  $B_x$  with nose 7.<sup>3</sup>

<sup>3</sup> If a propeller is operating at tip speeds near the velocity of sound, these efficiencies will, of course, be somewhat reduced by compressibility losses. The compressibility losses may be minimized by using thin propeller tip sections at or near the ideal angle of attack. (See reference 4.) Earlier experiments at the Laboratory (reference 5) have shown that sound velocity may be approached within 10 percent with no loss in efficiency.

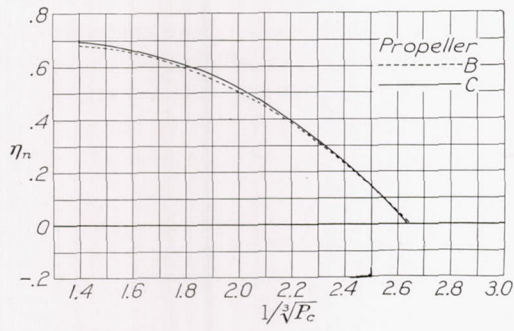


FIGURE 30.—Net-efficiency envelopes against  $1/\sqrt[3]{P_c}$  for propellers B and C on nose 1.

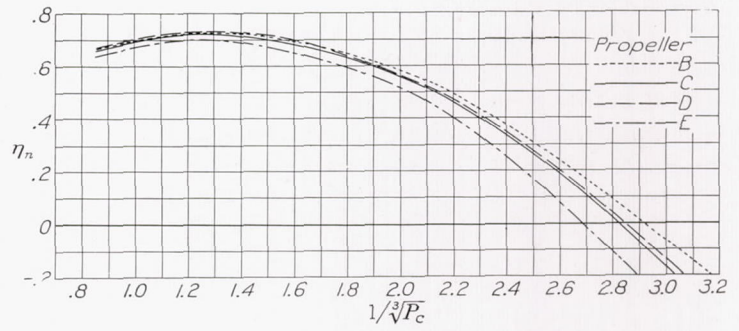


FIGURE 34.—Net-efficiency envelopes against  $1/\sqrt[3]{P_c}$  for propellers B, C, D, and E on nose 6.

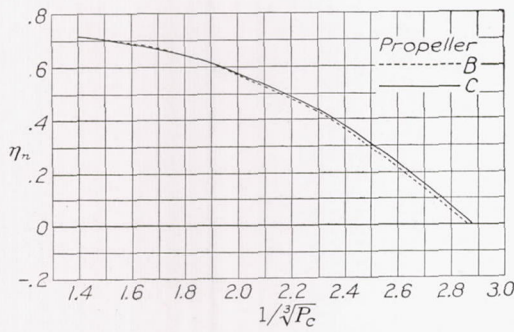


FIGURE 31.—Net-efficiency envelopes against  $1/\sqrt[3]{P_c}$  for propellers B and C on nose 2.

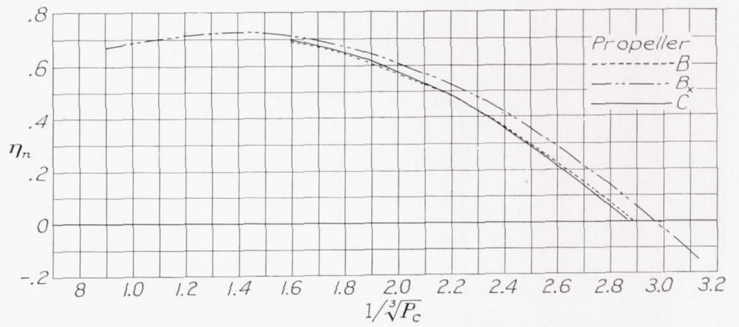


FIGURE 35.—Net-efficiency envelopes against  $1/\sqrt[3]{P_c}$  for propellers B, B<sub>x</sub>, and C on nose 7.

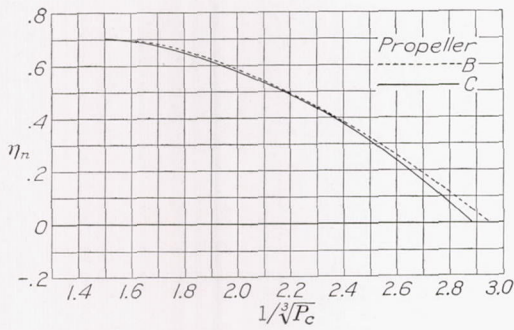


FIGURE 32.—Net-efficiency envelopes against  $1/\sqrt[3]{P_c}$  for propellers B and C on nose 3.

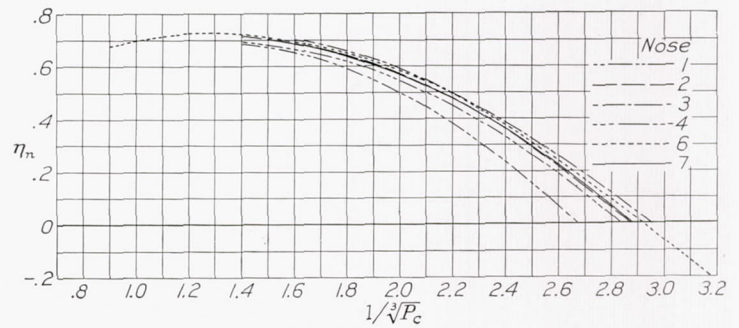


FIGURE 36.—Net-efficiency envelopes against  $1/\sqrt[3]{P_c}$  for noses 1, 2, 3, 4, 6, and 7 with propeller B.

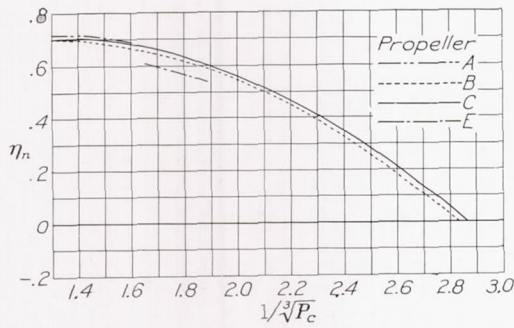


FIGURE 33.—Net-efficiency envelopes against  $1/\sqrt[3]{P_c}$  for propellers A, B, C, and E on nose 4.

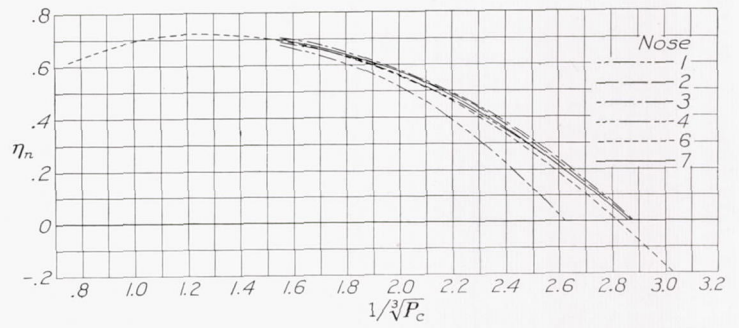


FIGURE 37.—Net-efficiency envelopes against  $1/\sqrt[3]{P_c}$  for noses 1, 2, 3, 4, 6, and 7 with propeller C.

Similarly, comparing net efficiencies for the most complete cases, cowlings 6 and 7, as given in figures 34 and 35, respectively, it is again seen that propeller B<sub>x</sub> is superior over most of the range. Notice also the marked improvement in the net efficiency of propeller B<sub>x</sub> as compared with that of its original form, B. Figure 36 for propeller B shows the superiority of noses

3 and 6 with 7 next. Since nose 3 gives poor cooling at low air speed, it should not be considered on an equal basis. Similar results for propeller C are shown in figure 37. This propeller is again less efficient than propeller B. Notice in both figures the very inferior efficiency of nose 1. Figure 38 has been included to show the cost of the cooling air as obtained by the standard skirt 2.

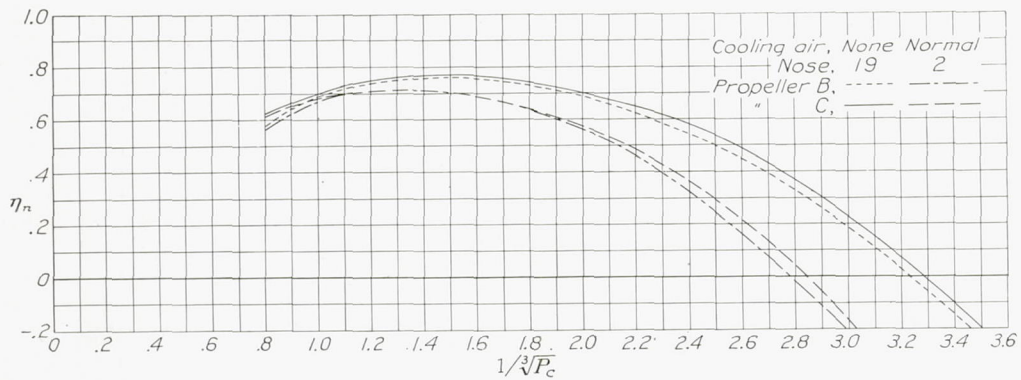


FIGURE 38.—Curves of net efficiency against  $1/\sqrt[3]{P_c}$  for propellers B and C set 25° at 0.75R; on nose 19, skirt 5, without cooling air; and on nose 2, skirt 2, with normal cooling air.

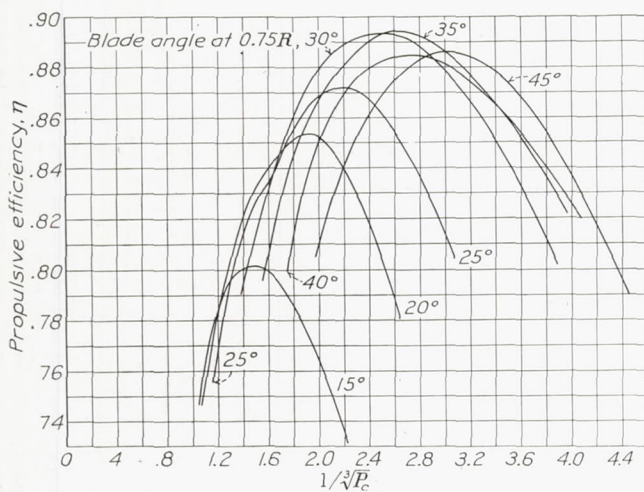


FIGURE 39.—Curves of propulsive efficiency against  $1/\sqrt[3]{P_c}$  for propeller B on nose 6.

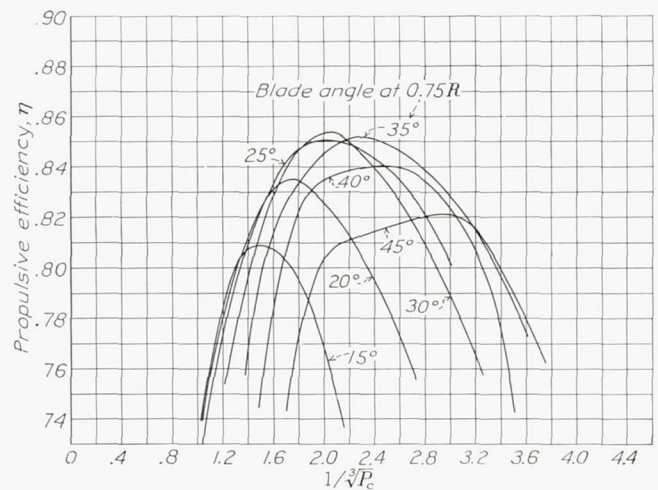


FIGURE 41.—Curves of propulsive efficiency against  $1/\sqrt[3]{P_c}$  for propeller C on nose 6.

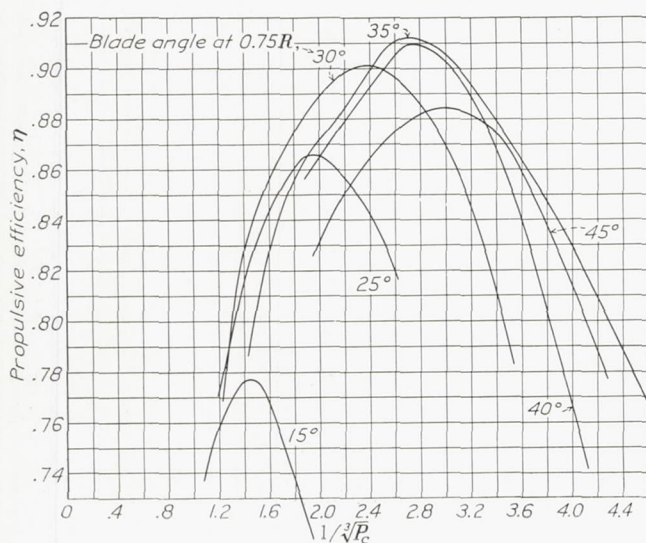


FIGURE 40.—Curves of propulsive efficiency against  $1/\sqrt[3]{P_c}$  for propeller B<sub>x</sub> on nose 7.

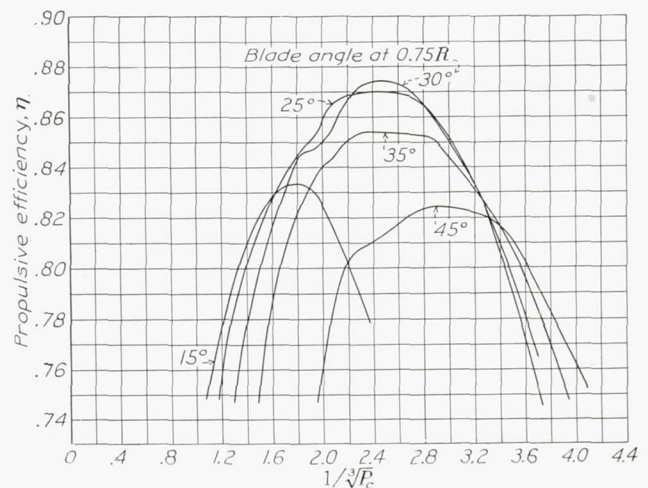


FIGURE 42.—Curves of propulsive efficiency against  $1/\sqrt[3]{P_c}$  for propeller D on nose 6.

In figures 39 to 42 the propulsive efficiency  $\eta$  has been plotted against  $1/\sqrt[3]{P_c}$  for propellers B, B<sub>x</sub>, C, and D. The envelopes for each of the five propellers are shown in figure 43. If the definition of  $P_c$  is recalled, it may be noted that with a fixed horsepower and a fixed propeller diameter the abscissa may be considered to represent the air speed. With a 550-horsepower engine and a 10-foot propeller, the abscissa happens to give the air speed in units of almost exactly 100 miles per hour. The propulsive efficiencies are compared at, say, 250 miles per hour. They are: Propeller B<sub>x</sub>, 90.9 percent; B, 89.4 percent; the two-blade propeller D, 87.4 percent; and propeller C, 84.9 percent, or a range of 6 percent. At lower speeds the differences are still of concern although less marked. It is of interest to note that the peak efficiencies of all propellers tested is found at a blade angle of approximately 35°.

The chart (fig. 43) is of value in demonstrating the fact that the present commonly used power plant of 550 horsepower in combination with a 10-foot propeller could be used to best advantage in the speed range 220 to 300 miles per hour. A 1,000-horsepower engine used on the same size propeller could be used to greatest advantage at about 25 percent higher speeds or in the range of 270 to 370 miles per hour. In order to make full use of a 1,000-horsepower engine at a speed

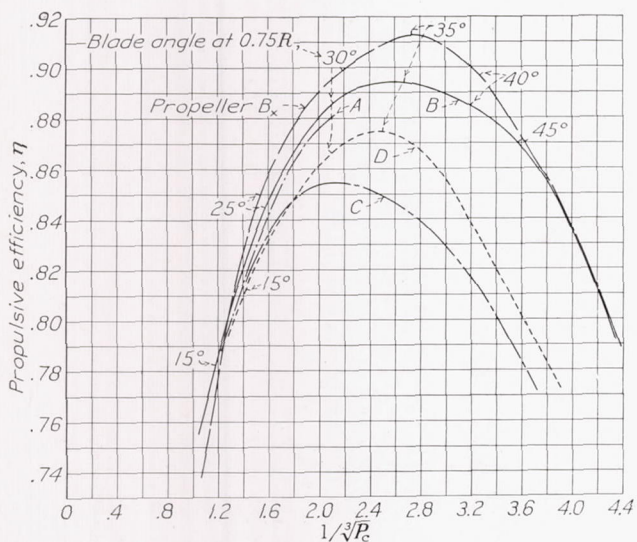


FIGURE 43.—Propulsive-efficiency envelopes against  $1/\sqrt[3]{P_c}$  for propellers A, B, B<sub>x</sub>, C, and D.

of 200 miles per hour, an impracticably large propeller diameter is required.

It also is of interest to note that the two-blade propeller D, employing the same blades as the three-blade propeller C, reaches a considerably greater peak efficiency. If 550 horsepower are used with both propellers, it is seen that the propulsive efficiencies at the speed of 250 miles per hour are, respectively, 87.4 and 84.9. This is a consequence of the fact that the commonly used propeller sections are altogether too wide. It was found that at the condition of peak efficiency of

the propeller, the actual or effective angle of attack amounts to only about 4° to 5°. It can be shown that a narrower blade with a correspondingly higher effective angle would be aerodynamically more efficient. Vibration and flutter and other considerations, however, prevent the practical use of such a blade.

Propellers B, C, and D all are designed with a constant blade angle for a setting of 12° at 0.75R. Propeller B<sub>x</sub> has a constant blade angle from 0.60R outward for a setting of 30° at 0.75R. (See fig. 3(a).)

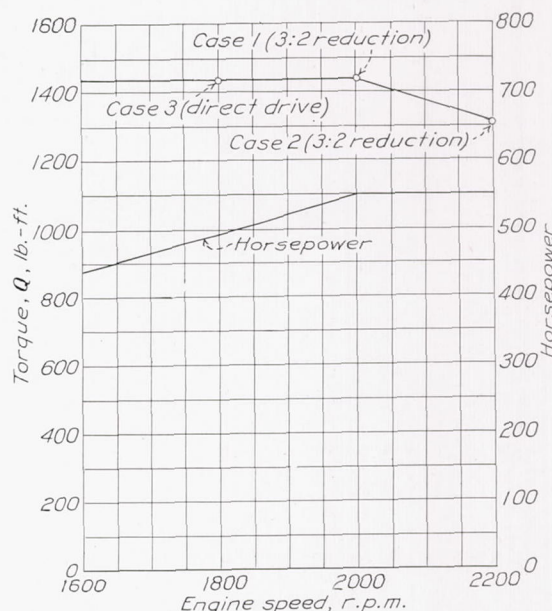


FIGURE 44.—Power and torque characteristics of an actual engine used as an example.

In fact, propeller B<sub>x</sub> is identical to propeller B except for this change in blade-angle distribution. The gain of almost 2 percent in efficiency observed in figure 43 demonstrates the importance of employing a design blade angle adjusted to the proper flight condition. Notice also that this gain is not obtained at the expense of decreased efficiency in the lower speed range. Propeller B<sub>x</sub> happens to be superior to all the propellers tested over the entire practical flight range.

The results of the tests of propellers B and C in conjunction with six different cowlings (figs. 36 and 37) illustrate the importance of the effect of the cowling. Considering the somewhat fictitious case of the top speed attainable with the present nacelle alone, it is observed in figure 36 that the comparative top speeds range from 267 miles per hour for nose 1 to 295 miles per hour for nose 3. For propeller C (fig. 37) the comparative range is 262 miles to 288 miles. Although the differences between the cowlings of reasonable design are fairly small, the inferiority of a design resembling nose 1 should be kept in mind, this nose being the cause of a speed reduction of almost 10 percent.

**TAKE-OFF CHARACTERISTICS**

The propeller characteristics at low air speeds may be obtained from the basic test results given in figures 5 to 22. In order to make full use of this information

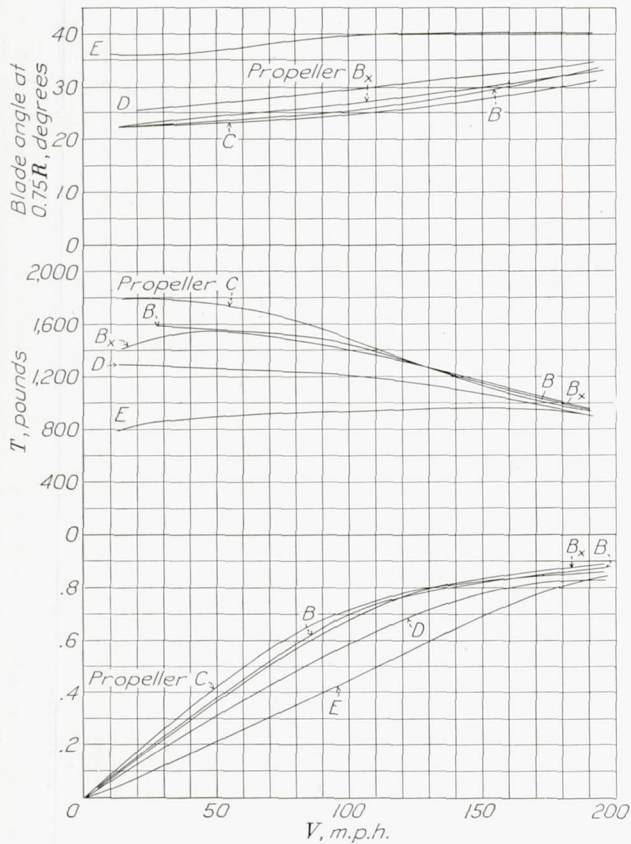


FIGURE 45.—Optimum blade angle and thrust in the take-off range, engine speed 2,000 revolutions per minute, with a 3:2 gear reduction ratio.

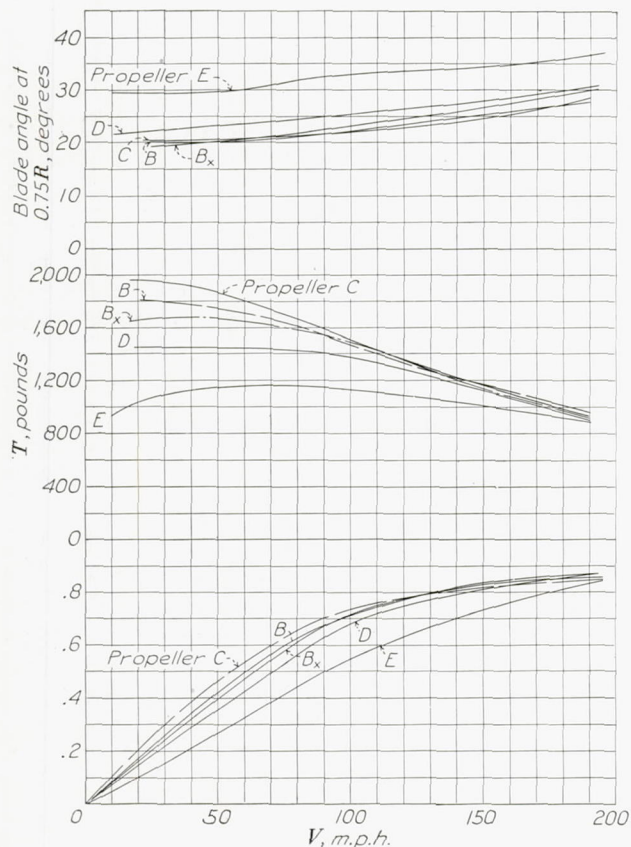


FIGURE 46.—Optimum blade angle and thrust in the take-off range, engine speed 2,200 revolutions per minute with a 3:2 gear reduction ratio.

in calculating the take-off distance for a given set of conditions, however, it is necessary to present the data in a more direct manner. The optimum blade-angle setting corresponding to the maximum available thrust at any particular air speed is of particular interest.

The actual differences in the take-off characteristics will be directly demonstrated by the use of a particular example using engine characteristics as given in figure 44 corresponding to those actually obtained on a 550-horsepower engine. The engine speeds chosen are: 2,000 revolutions per minute and 2,200 revolutions per minute, both with a 3:2 gear reduction ratio; and 1,800 revolutions per minute with direct drive.

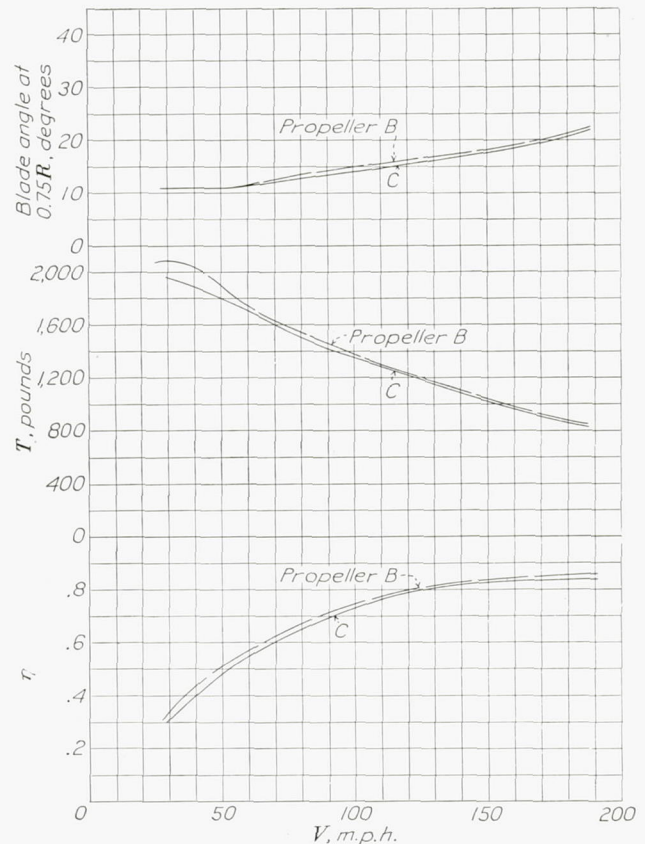


FIGURE 47.—Optimum blade angle and thrust in the take-off range, engine speed 1,800 revolutions per minute with direct drive.

The resulting blade-angle settings and thrusts in the take-off range obtained from charts in the appendix are presented in figures 45, 46, and 47. It is noticed in working through one of these examples that no particular optimum setting is reached; the maximum permissible engine speed is the limiting condition. Notice that propeller C is very superior to B or B<sub>x</sub> in regard to take-off, particularly in the lowest speed range.<sup>4</sup> The thrust of the two-blade propeller D is further seen to amount to a little more than two-thirds of that of the corresponding three-blade propeller C. Propeller B<sub>x</sub> is noticed to be slightly inferior to propeller

<sup>4</sup> This comparison is valid when propellers of a constant diameter are being compared, as would be the case when the propeller diameter is the limiting design factor. Given a free choice of diameters, the comparisons must be made with a view to the high-speed performance, necessitating an individual study of each case.

B at speeds less than about 100 miles per hour. Notice the inferior thrust values of the 9-foot propeller E. Absorbing the same horsepower, this propeller is relatively overloaded and should not be directly compared. The beneficial influence of increasing the propeller speed may be observed by comparing the results from the three figures.

The results are, of course, strictly true only for the relative dimensions of the propeller and nacelle used in these particular experiments, a larger propeller thus calling for a larger nacelle, and vice versa. It is, however, known that the propulsive efficiency will be affected very little by this variation in relative dimensions. The results may, therefore, be considered valid also for the case of different relative dimensions of the propeller in regard to the nacelle.

As these propellers are fairly representative of commonly used types, it is possible by some exercise of judgment to obtain a fairly reasonable estimate of the take-off characteristics also of any other propellers.

GENERAL CONCLUSIONS

1. Peak efficiency of the propellers tested occurs at a blade-angle setting of approximately 35°. The difference in peak efficiency varies as much as 6 percent, demonstrating the value of selecting a good design, particularly in the high-speed range.

2. The peak propulsive efficiency of the conventionally dimensional units of 9- to 12-foot propellers on 500- to 1,000-horsepower engines has been found to lie in the range of 200 to 350 miles per hour, showing the beneficial influence of higher air speeds on the propeller.

3. A two-blade propeller of the kind tested was found to be superior in efficiency (in the high-speed range) to a three-blade propeller using identical blades, the peak efficiency exceeding that of the three-blade propeller by about 2 percent.

4. A propeller equipped with a controllable hub shows an almost negligible decrease in efficiency as compared with the identical propeller with a standard hub. The difference is of the order of ½ percent, which is close to the limit of test accuracy.

5. In regard to the take-off characteristics, the maximum permissible revolution speed is in all cases found to be the most favorable. The three-blade propeller is superior to the two-blade propeller using the same horsepower, which is to be expected.

LANGLEY MEMORIAL AERONAUTICAL LABORATORY,  
NATIONAL ADVISORY COMMITTEE FOR AERONAUTICS,  
LANGLEY FIELD, VA., June 4, 1936.

LIST OF SYMBOLS

$V$	Velocity of air stream
$n$	Revolutions per unit time of the propeller
$D$	Diameter of propeller
$\frac{V}{nD}$	Advance-diameter ratio of the propeller
$P$	Power supplied to propeller shaft
$S$	Disk area of propeller
$q$	Velocity head of air stream, $\frac{1}{2} \rho V^2$
$P_c = \frac{P}{qSV}$	Unit disk loading or disk-loading coefficient
$\rho$	Air density
$R$	Net forward thrust of the entire unit as measured on the thrust scale
$\eta_n = \frac{RV}{P}$	Net efficiency
$T = R + D$	Thrust
$D$	Drag of the nacelle unit for the corresponding air speed measured with the propeller off
$C_T = \frac{T}{\rho n^2 D^4}$	Thrust coefficient
$\frac{1}{\sqrt[3]{P_c}} = V \sqrt[3]{\frac{\rho S}{2P}}$	
$C_P = \frac{P}{\rho n^3 D^5}$	Power coefficient
$C_Q = \frac{Q}{\rho n^2 D^5}$	Torque coefficient
$\eta = \frac{TV}{P}$	Propulsive efficiency
$Q$	Torque of propeller
$Q_c = \frac{Q}{\rho V^2 D^3}$	Torque coefficient
$h$	Thickness of blade section of propeller
$b$	Width of blade section of propeller
$r$	Radius to any blade section of propeller
$R$	Radius of propeller
$\beta$	Propeller blade-angle setting at $0.75 R$
$P$	Geometric pitch of propeller
$C_S = \sqrt[5]{\frac{\rho V^5}{P n^2}}$	Speed-power coefficient
$\eta_0$	Net propeller-nacelle efficiency with no cooling air

## APPENDIX

### CHARTS FOR SELECTING PROPELLER DIAMETERS

The characteristics of a propeller are given as a relation of three and only three variables; these variables may be given as  $C_T$ ,  $C_P$ ,  $V/nD$ . For geometrically similar propellers these quantities remain constant. Any other three independent variables may be selected, and the combination of  $C_s$ ,  $V/nD$ , and  $\eta$  is chosen because of certain advantages. Since only three quantities are involved, it is obviously possible to give a complete representation of the characteristics in a single contour chart. Inserting values of the efficiency  $\eta$  against  $C_s$  as ordinates and  $V/nD$  as abscissas for various blade-angle settings, connecting points of equal efficiencies and points representing given blade angles, gives a contour map containing all results. This type of chart is primarily useful in selecting the diameter of a propeller. It is tacitly assumed that the type of propeller has already been chosen and that charts are available. It is interesting to observe that the contour lines map a smoothly shaped peak; no crowding of the lines occurs. In the selection of a propeller diameter this type of chart makes it possible to judge the effect of changes by observing how the representative point moves with respect to the efficiency peak.

Charts I give the results for the three-blade propeller B, the modified version B<sub>x</sub>, C, and the two-blade propeller D. The charts are applicable to controllable propellers allowing for 1/2 percent decrease in efficiency by a slight increase in the diameter.

#### PROCEDURE FOR THE USE OF CONTOUR CHARTS FOR SELECTING PROPELLER DIAMETERS

Given: Horsepower  $P$ , revolutions per second  $n$ , air speed  $V$ , and density  $\rho$ .

Calculate:

$$C_s = V \sqrt[5]{\frac{\rho}{Pn^2}}$$

(1) For a controllable-pitch propeller, select the point of maximum efficiency at this value of  $C_s$ . (The efficiency envelope is shown by a curve on the chart.) Read off angle setting and  $V/nD$ , the latter giving the value of  $D$ .<sup>1</sup>

Examples are shown on the particular charts.

(2) For a fixed-pitch propeller the selection of the blade-angle setting is a matter of compromise. It is necessary to choose a blade angle that shows peak efficiency at a somewhat smaller value of  $C_s$  than the one calculated for the flight condition. The choice depends on how much efficiency is to be sacrificed at the high-speed condition in order to improve the take-off. It is therefore necessary to resort to the simultaneous use of charts giving the take-off characteristics.

<sup>1</sup> Notice that the blade-angle setting in the charts is the true setting at the operating condition. The results presented are free from compressibility effects and twist of blades due to air loads and the effect of the centrifugal force. The blade twist can be estimated and allowed for.

### CHARTS FOR THE TAKE-OFF CONDITION

In the determination of the diameter of a propeller, consideration must be given also to the condition of take-off. It is desirable to know the thrust in order to calculate the take-off distance. For the controllable-pitch propeller, the determination of the minimum blade-angle setting is of interest. For the fixed-pitch propeller, the setting is a matter of balancing the performance at high speed against that at take-off. It will probably be necessary to study two or three blade-angle settings in order to arrive at a specific result. Charts for determining the take-off thrust, based on the results of this investigation, are given in charts II as supplements to charts I already described. These charts, which have been developed along similar lines, show contour curves of constant thrust and constant blade-angle setting against the coordinates  $V/nD$  and  $1/\sqrt{Q_c} = V \sqrt{\frac{\rho D^3}{Q}}$ , the latter quantity representing a torque coefficient; the actual engine torque  $Q$  is, as usual, considered to be a constant. Results are given in charts II.

#### PROCEDURE FOR THE USE OF CHARTS ON TAKE-OFF CHARACTERISTICS

(1) Controllable-pitch propeller.

Given: Engine torque  $Q$ , propeller diameter  $D$ , revolutions per second  $n$ , and air speed  $V$ .

Calculate  $1/\sqrt{Q_c}$  and  $V/nD$ .

Read off from the chart  $C_T/C_Q = TD/Q$  and the blade angle. For constant  $n$  the whole range of air speed is given by a straight line through this point and the origin. Plot thrust and blade angle against air speed (as in fig. 45, etc.).

(2) Fixed-pitch propeller

Calculate  $1/\sqrt{Q_c}$  and  $V/nD$ .

Make a choice of blade angle and read from the chart the related values of  $C_T/C_Q$  and  $1/\sqrt{Q_c}$ . Plot thrust against air speed for this blade angle. If the resulting take-off thrust is found to be inadequate, choose a lower blade angle and repeat the procedure; or vice versa.

#### REFERENCES

1. Theodorsen, Theodore, Brevoort, M. J., and Stickle, George W.: Full-scale Tests of N. A. C. A. Cowlings. T. R. No. 592, N. A. C. A., 1937.
2. Theodorsen, Theodore, Brevoort, M. J., and Stickle, George W.: Cooling of Airplane Engines at Low Air Speeds. T. R. No. 593, N. A. C. A., 1937.
3. Weick, Fred E., and Wood, Donald H.: The Twenty-Foot Propeller Research Tunnel of the National Advisory Committee for Aeronautics. T. R. No. 300, N. A. C. A., 1928.
4. Theodorsen, Theodore: On the Theory of Wing Sections with Particular Reference to the Lift Distribution. T. R. No. 383, N. A. C. A., 1931.
5. Wood, Donald H.: Full-Scale Tests of Metal Propellers at High Tip Speeds. T. R. No. 375, N. A. C. A., 1931.

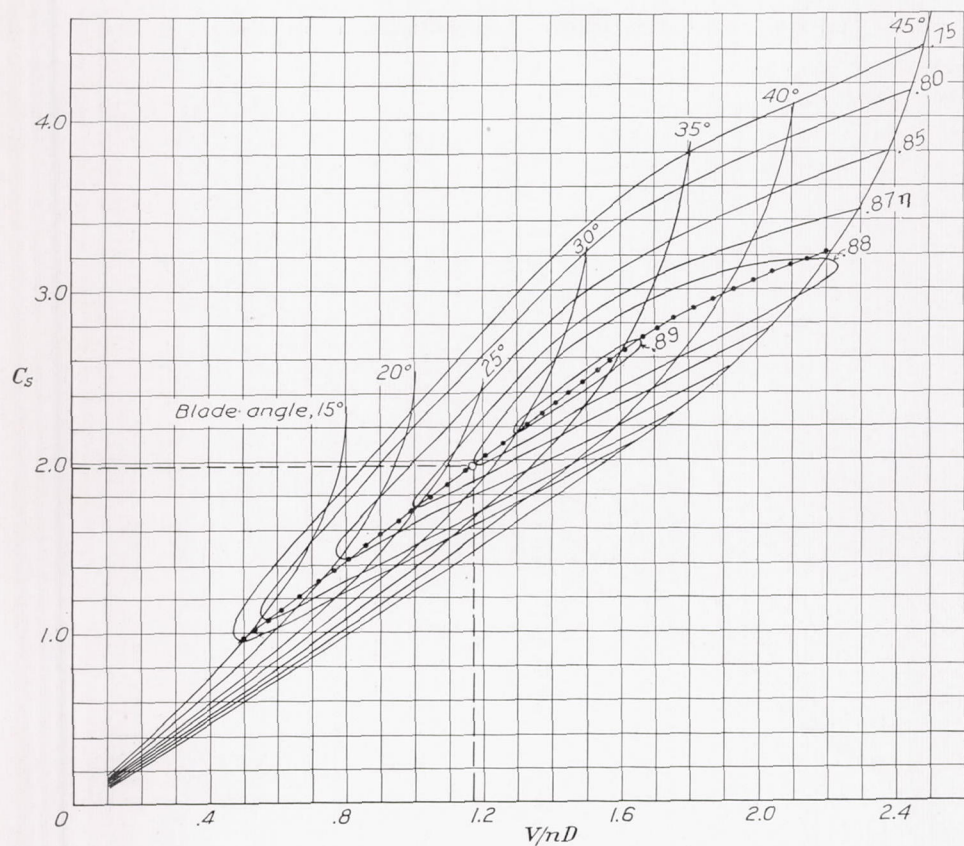


CHART I (a).—Characteristics of three-blade propeller B. Hamilton-Standard 1C1-0. Example (shown by circle)—Given:  $P=550$  horsepower;  $n=24$  revolutions per second;  $V=200$  miles per hour. Result:  $\beta=27^\circ$ ;  $\eta=0.877$ ;  $D=10.68$  feet.

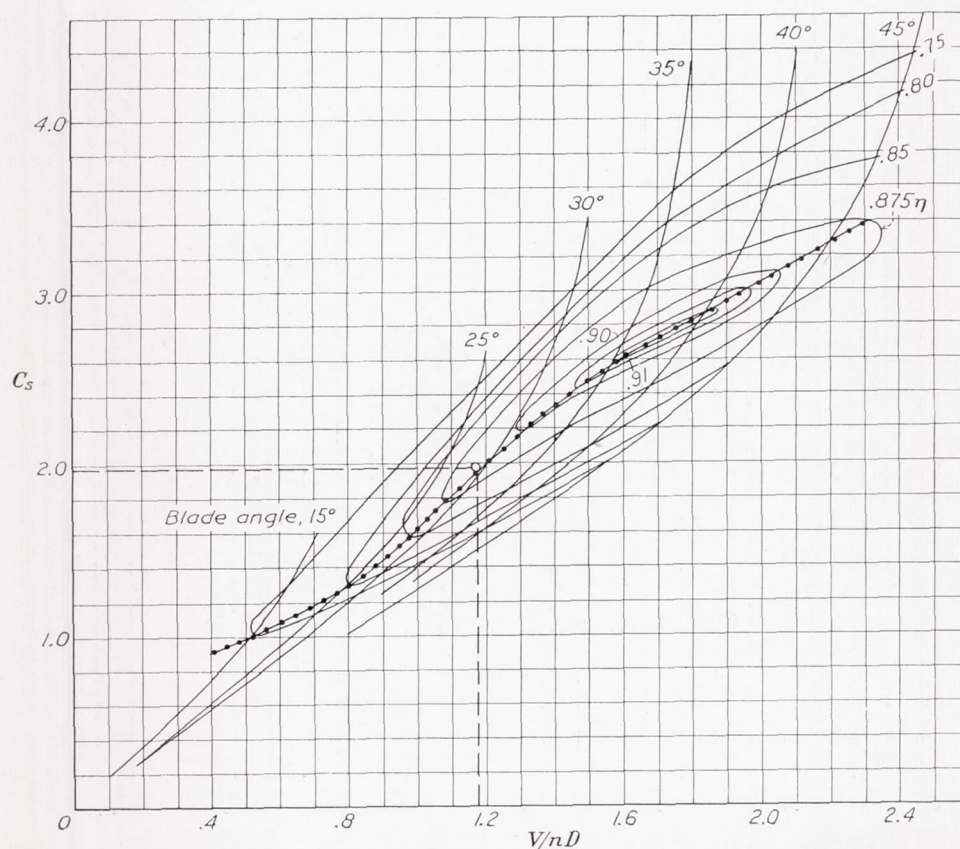


CHART I (b).—Characteristics of three-blade propeller Bx. Hamilton-Standard 1C1-0 (modified). Example (shown by circle)— Given:  $P=550$  horsepower;  $n=24$  revolutions per second;  $V=200$  miles per hour. Result:  $\beta=29^\circ$ ;  $\eta=0.883$ ;  $D=10.44$  feet.

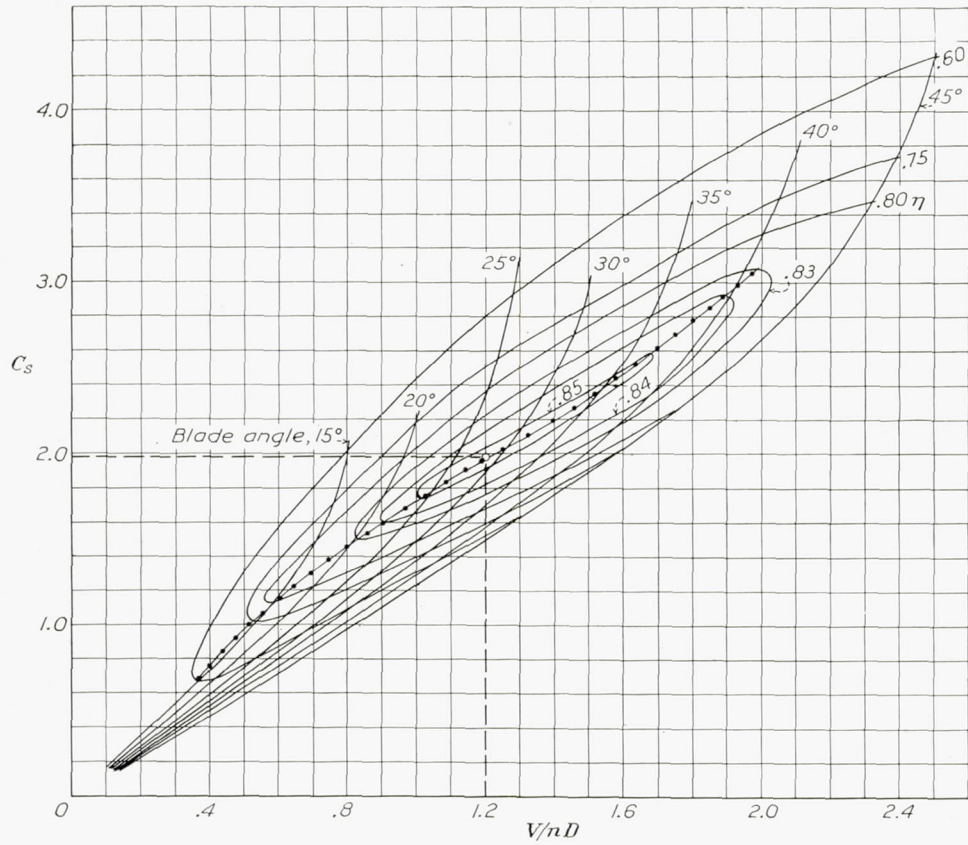


CHART I (c).—Characteristics of three-blade propeller C. Navy plan form 5868-9. Example (shown by circle)—Given:  $P=550$  horsepower;  $n=24$  revolutions per second;  $V=200$  miles per hour. Result:  $\beta=28.3^\circ$ ;  $\eta=0.855$ ;  $D=10.18$  feet.



CHART I (d).—Characteristics of two-blade propeller D. Navy plan form 5868-9. Example (shown by circle)—Given:  $P=550$  horsepower;  $n=24$  revolutions per second;  $V=200$  miles per hour. Result:  $\beta=25^\circ$ ;  $\eta=0.865$ ;  $D=11.50$  feet.

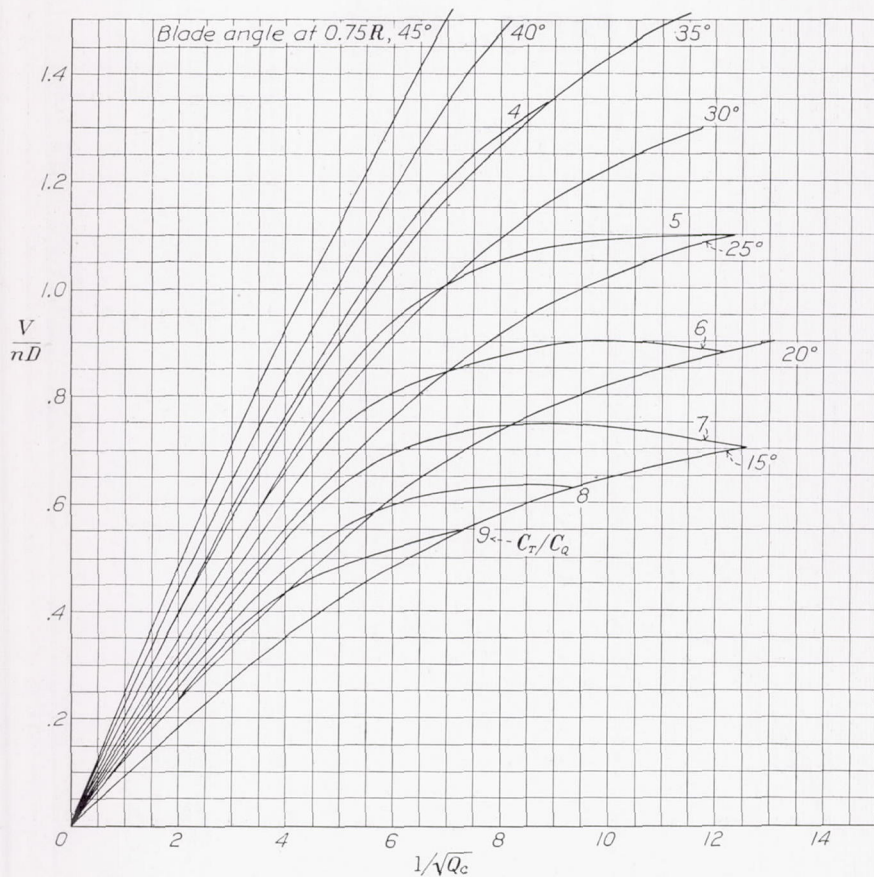


CHART II (a).—Take-off characteristics for three-blade propeller B. Hamilton-Standard 1C1-0.

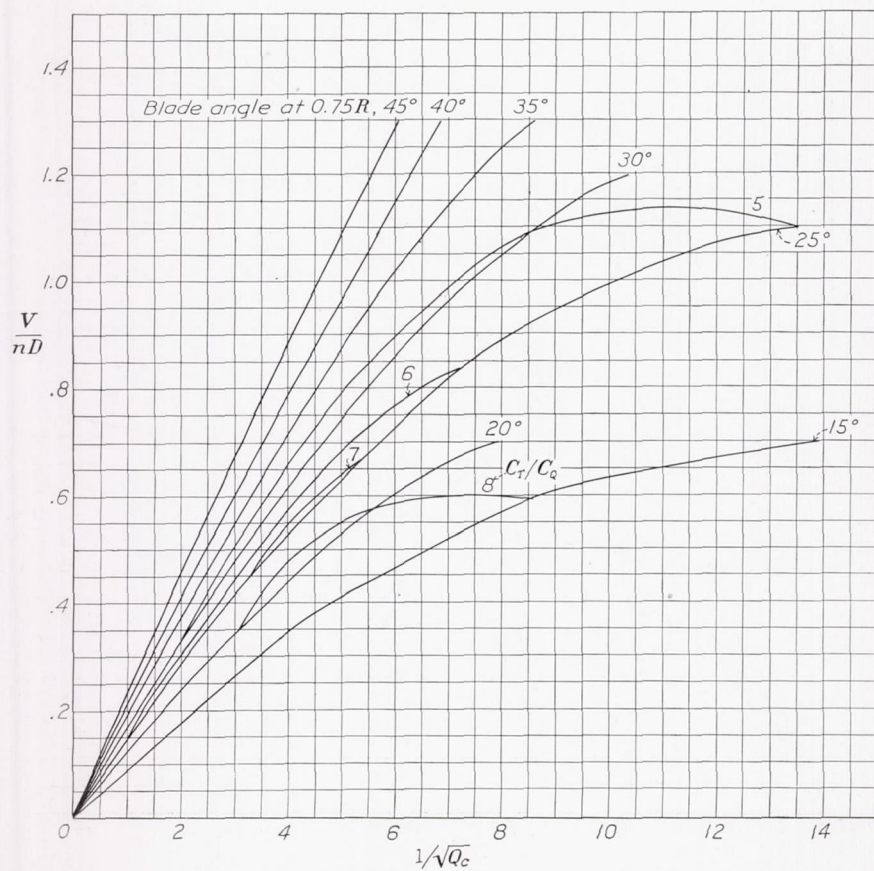


CHART II (b).—Take-off characteristics for three-blade propeller Bx. Hamilton-Standard 1C1-0 (modified).

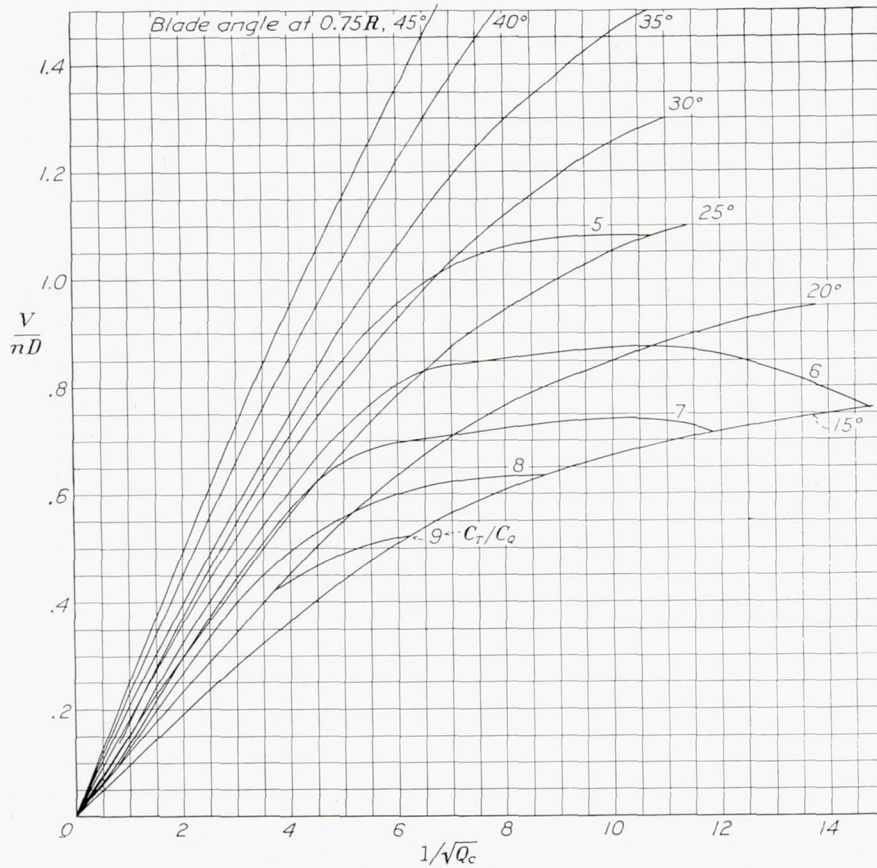


CHART II (c).—Take-off characteristics for three-blade propeller C. Navy plan form 5868-9.

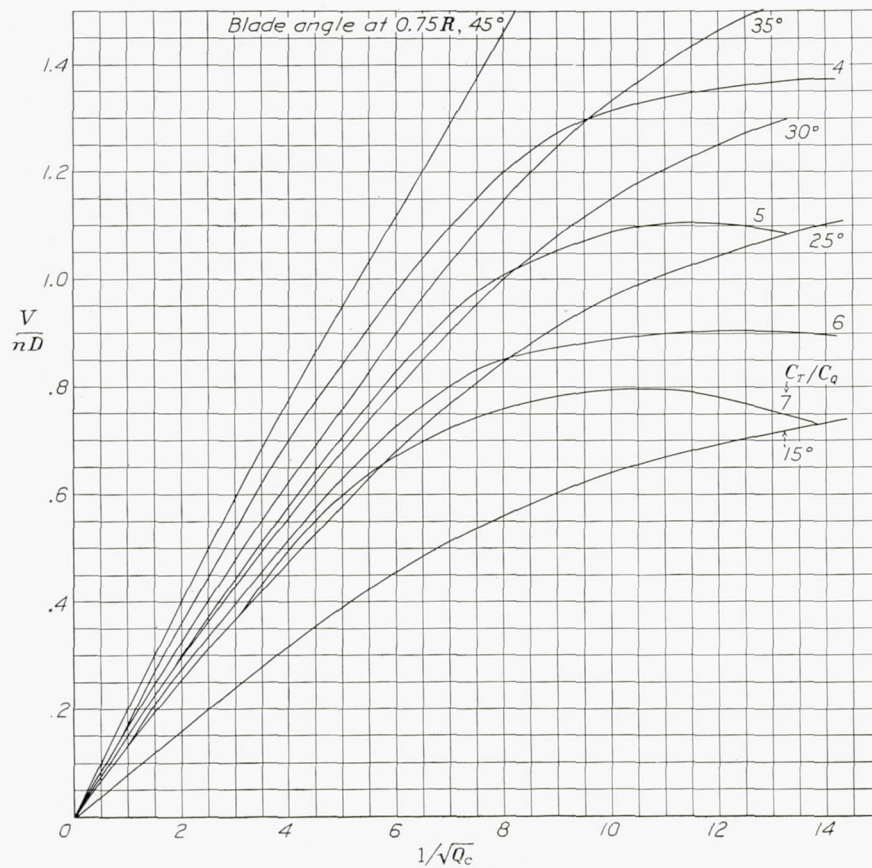


CHART II (d).—Take-off characteristics for two-blade propeller D. Navy plan form 5868-9.



TABLE I.—FAIRED VALUES FOR NOSE 6, PROPELLER B—Continued

$V/nD$	Set 35° at 0.75R				Set 40° at 0.75R				Set 45° at 0.75R			
	$C_T$	$C_P$	$\eta$	$C_S$	$C_T$	$C_P$	$\eta$	$C_S$	$C_T$	$C_P$	$\eta$	$C_S$
0	0.1635	0.2695	0	0	0.1643	0.3324	0	0	0.1576	0.3868	0	0
.05	.1629	.2662	.031	.07	.1640	.3291	.025	.06	.1581	.3842	.021	.06
.10	.1617	.2631	.062	.13	.1637	.3260	.050	.13	.1585	.3817	.042	.12
.15	.1606	.2600	.093	.20	.1633	.3228	.076	.19	.1589	.3792	.063	.18
.20	.1593	.2567	.124	.26	.1628	.3197	.102	.25	.1592	.3767	.085	.24
.25	.1583	.2535	.156	.33	.1624	.3164	.128	.32	.1596	.3742	.106	.30
.30	.1570	.2501	.188	.40	.1618	.3132	.155	.38	.1599	.3717	.129	.37
.35	.1557	.2467	.221	.46	.1613	.3100	.182	.44	.1602	.3693	.152	.43
.40	.1543	.2432	.254	.53	.1607	.3067	.210	.51	.1605	.3667	.175	.49
.45	.1530	.2396	.288	.60	.1600	.3033	.238	.57	.1608	.3640	.199	.55
.50	.1517	.2360	.322	.67	.1593	.3000	.266	.64	.1607	.3614	.222	.61
.55	.1502	.2323	.356	.74	.1585	.2963	.294	.70	.1605	.3586	.246	.68
.60	.1490	.2285	.391	.81	.1577	.2927	.323	.77	.1601	.3557	.270	.74
.65	.1475	.2245	.427	.88	.1566	.2890	.352	.83	.1596	.3527	.294	.80
.70	.1462	.2205	.464	.95	.1554	.2853	.381	.90	.1588	.3499	.318	.86
.75	.1445	.2165	.500	1.02	.1542	.2813	.412	.97	.1577	.3466	.341	.93
.80	.1427	.2121	.538	1.09	.1527	.2770	.441	1.03	.1565	.3434	.365	.99
.85	.1405	.2078	.575	1.17	.1510	.2730	.470	1.10	.1550	.3400	.388	1.05
.90	.1375	.2028	.610	1.24	.1492	.2683	.500	1.17	.1538	.3362	.411	1.12
.95	.1345	.1982	.645	1.31	.1470	.2634	.530	1.25	.1522	.3324	.435	1.19
1.00	.1317	.1940	.678	1.39	.1445	.2580	.560	1.31	.1507	.3277	.460	1.25
1.05	.1290	.1895	.715	1.47	.1418	.2530	.589	1.38	.1490	.3232	.484	1.32
1.10	.1255	.1841	.750	1.54	.1392	.2490	.615	1.45	.1475	.3183	.510	1.38
1.15	.1202	.1777	.779	1.62	.1372	.2455	.643	1.52	.1460	.3135	.536	1.45
1.20	.1140	.1700	.804	1.71	.1355	.2428	.670	1.59	.1443	.3088	.560	1.52
1.25	.1067	.1624	.820	1.80	.1340	.2400	.698	1.66	.1428	.3052	.585	1.59
1.30	.0993	.1533	.842	1.89	.1324	.2360	.730	1.74	.1412	.3015	.610	1.65
1.35	.0913	.1440	.855	1.99	.1300	.2310	.760	1.81	.1398	.2990	.631	1.72
1.40	.0830	.1340	.867	2.09	.1267	.2255	.796	1.89	.1385	.2964	.655	1.79
1.45	.0750	.1240	.876	2.20	.1215	.2185	.805	1.96	.1371	.2948	.675	1.85
1.50	.0658	.1117	.884	2.32	.1157	.2103	.825	2.05	.1360	.2925	.698	1.92
1.55	.0570	.0990	.893	2.46	.1090	.2010	.841	2.13	.1348	.2904	.720	1.98
1.60	.0478	.0850	.900	2.62	.1020	.1910	.855	2.23	.1339	.2878	.745	2.05
1.65	.0385	.0712	.892	2.80	.0940	.1790	.866	2.32	.1324	.2845	.767	2.12
1.70	.0288	.0558	.876	3.03	.0858	.1670	.873	2.42	.1303	.2805	.790	2.20
1.75	.0195	.0400	.853	3.33	.0770	.1540	.875	2.54	.1270	.2760	.805	2.27
1.80	.0100	.0237	.760	3.80	.0685	.1400	.881	2.66	.1220	.2690	.816	2.34
1.85	.0007	.0078	.166	4.88	.0595	.1240	.888	2.81	.1160	.2590	.829	2.42
1.90	-----	-----	-----	-----	.0500	.1080	.880	2.96	.1095	.2480	.839	2.51
1.95	-----	-----	-----	-----	.0410	.0915	.874	3.14	.1030	.2353	.855	2.60
2.00	-----	-----	-----	-----	.0320	.0745	.860	3.36	.0950	.2220	.855	2.70
2.05	-----	-----	-----	-----	.0230	.0575	.810	3.63	.0876	.2080	.863	2.80
2.10	-----	-----	-----	-----	.0147	.0400	.771	4.00	.0800	.1920	.874	2.92
2.15	-----	-----	-----	-----	.0058	.0220	.566	4.61	.0714	.1750	.877	3.05
2.20	-----	-----	-----	-----	.0025	.0038	-----	6.70	.0632	.1580	.880	3.18
2.25	-----	-----	-----	-----	-----	-----	-----	-----	.0550	.1400	.883	3.30
2.30	-----	-----	-----	-----	-----	-----	-----	-----	.0470	.1230	.878	3.50
2.35	-----	-----	-----	-----	-----	-----	-----	-----	.0387	.1050	.867	3.69
2.40	-----	-----	-----	-----	-----	-----	-----	-----	.0305	.0870	.842	3.91
2.45	-----	-----	-----	-----	-----	-----	-----	-----	.0228	.0688	.812	4.18
2.50	-----	-----	-----	-----	-----	-----	-----	-----	.0150	.0505	.742	4.53
2.55	-----	-----	-----	-----	-----	-----	-----	-----	.0070	.0320	.558	4.81
2.60	-----	-----	-----	-----	-----	-----	-----	-----	.0005	.0140	-----	6.10



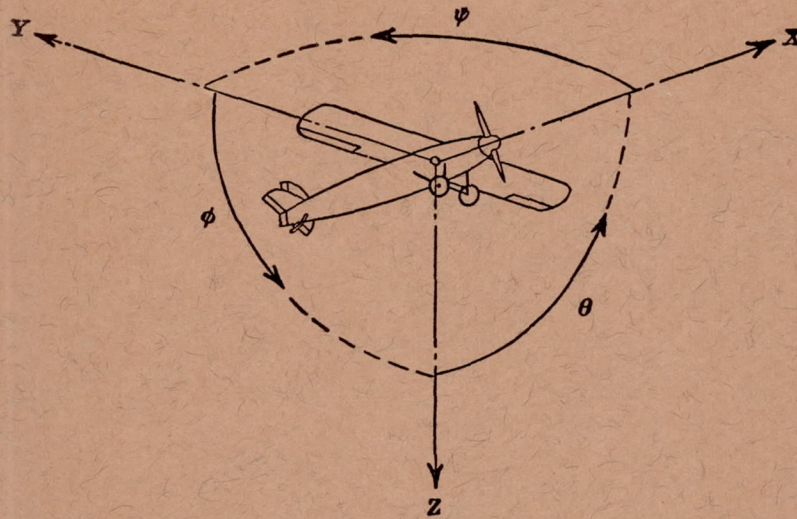
TABLE II.—FAIRED VALUES FOR NOSE 7, PROPELLER B<sub>x</sub>—Continued

V/nD	Set 35° at 0.75R				Set 40° at 0.75R				Set 45° at 0.75R			
	C <sub>T</sub>	C <sub>P</sub>	η	C <sub>S</sub>	C <sub>T</sub>	C <sub>P</sub>	η	C <sub>S</sub>	C <sub>T</sub>	C <sub>P</sub>	η	C <sub>S</sub>
0	0.1515	0.2468	0	0	0.1492	0.2970	0	0	0.1456	0.3490	0	0
.05	.1508	.2440	.031	.07	.1490	.2930	.025	.06	.1460	.3480	.021	.06
.10	.1500	.2410	.062	.13	.1484	.2890	.051	.13	.1462	.3465	.042	.12
.15	.1490	.2381	.094	.20	.1480	.2850	.078	.19	.1465	.3450	.064	.19
.20	.1480	.2351	.126	.27	.1473	.2810	.105	.26	.1468	.3435	.086	.25
.25	.1470	.2292	.160	.34	.1470	.2773	.133	.32	.1470	.3420	.107	.31
.30	.1460	.2263	.194	.41	.1463	.2734	.161	.39	.1470	.3405	.129	.37
.35	.1448	.2233	.227	.47	.1457	.2695	.189	.46	.1470	.3385	.152	.44
.40	.1435	.2202	.260	.54	.1450	.2658	.217	.52	.1470	.3370	.175	.50
.45	.1423	.2170	.295	.61	.1443	.2625	.248	.59	.1470	.3350	.197	.56
.50	.1410	.2140	.330	.68	.1435	.2590	.278	.66	.1470	.3330	.221	.62
.55	.1397	.2105	.365	.75	.1429	.2560	.307	.72	.1470	.3308	.244	.69
.60	.1382	.2074	.400	.82	.1420	.2530	.337	.79	.1468	.3283	.268	.75
.65	.1365	.2040	.435	.89	.1410	.2500	.367	.86	.1464	.3255	.292	.81
.70	.1348	.2004	.470	.97	.1400	.2472	.397	.93	.1460	.3220	.318	.88
.75	.1333	.1972	.507	1.04	.1390	.2445	.427	1.00	.1455	.3185	.343	.94
.80	.1325	.1944	.545	1.11	.1380	.2420	.456	1.06	.1448	.3148	.368	1.01
.85	.1325	.1920	.586	1.18	.1368	.2400	.485	1.13	.1440	.3110	.394	1.07
.90	.1330	.1897	.630	1.26	.1353	.2378	.512	1.20	.1429	.3075	.418	1.14
.95	.1325	.1855	.679	1.33	.1338	.2356	.545	1.27	.1415	.3043	.441	1.21
1.00	.1315	.1800	.730	1.41	.1328	.2335	.569	1.34	.1401	.3013	.465	1.28
1.05	.1293	.1800	.754	1.48	.1325	.2317	.601	1.41	.1384	.2985	.487	1.34
1.10	.1250	.1740	.791	1.56	.1331	.2300	.637	1.48	.1370	.2960	.510	1.40
1.15	.1181	.1670	.813	1.64	.1334	.2282	.671	1.55	.1358	.2938	.532	1.47
1.20	.1110	.1600	.833	1.73	.1335	.2258	.710	1.62	.1350	.2918	.555	1.53
1.25	.1033	.1525	.846	1.82	.1330	.2215	.750	1.69	.1343	.2901	.578	1.60
1.30	.0955	.1445	.853	1.92	.1310	.2163	.787	1.77	.1340	.2889	.603	1.67
1.35	.0870	.1360	.864	2.01	.1270	.2105	.815	1.84	.1343	.2880	.629	1.73
1.40	.0785	.1260	.872	2.12	.1213	.2044	.830	1.92	.1349	.2875	.655	1.80
1.45	.0698	.1147	.881	2.24	.1150	.1976	.844	2.00	.1359	.2870	.686	1.87
1.50	.0610	.1023	.895	2.36	.1086	.1900	.857	2.08	.1365	.2858	.717	1.93
1.55	.0520	.0890	.905	2.51	.1018	.1820	.866	2.18	.1365	.2830	.747	2.00
1.60	.0428	.0745	.918	2.69	.0940	.1730	.870	2.28	.1353	.2783	.777	2.07
1.65	.0333	.0600	.915	2.89	.0864	.1620	.880	2.38	.1324	.2723	.801	2.14
1.70	.0230	.0450	.869	3.16	.0785	.1500	.890	2.48	.1280	.2650	.821	2.22
1.75	.0135	.0290	.814	3.56	.0700	.1367	.896	2.60	.1225	.2575	.832	2.30
1.80	.0040	.0123	.585	4.33	.0620	.1225	.911	2.74	.1167	.2495	.842	2.38
1.85	-----	-----	-----	-----	.0530	.1080	.908	2.89	.1100	.2400	.848	2.46
1.90	-----	-----	-----	-----	.0440	.0930	.900	3.05	.1030	.2282	.858	2.56
1.95	-----	-----	-----	-----	.0350	.0782	.873	3.24	.0950	.2150	.862	2.66
2.00	-----	-----	-----	-----	.0260	.0630	.825	3.48	.0870	.2010	.865	2.76
2.05	-----	-----	-----	-----	.0170	.0465	.749	3.88	.0790	.1853	.874	2.87
2.10	-----	-----	-----	-----	.0078	.0270	.607	4.32	.0713	.1700	.880	2.99
2.15	-----	-----	-----	-----	-.0013	.0060	-----	5.99	.0632	.1535	.886	3.13
2.20	-----	-----	-----	-----	-----	-----	-----	-----	.0554	.1380	.883	3.27
2.25	-----	-----	-----	-----	-----	-----	-----	-----	.0470	.1205	.879	3.44
2.30	-----	-----	-----	-----	-----	-----	-----	-----	.0393	.1040	.870	3.62
2.35	-----	-----	-----	-----	-----	-----	-----	-----	.0310	.0870	.836	3.82
2.40	-----	-----	-----	-----	-----	-----	-----	-----	.0231	.0695	.797	4.09
2.45	-----	-----	-----	-----	-----	-----	-----	-----	.0150	.0500	.735	4.45
2.50	-----	-----	-----	-----	-----	-----	-----	-----	.0070	.0295	.593	5.05
2.55	-----	-----	-----	-----	-----	-----	-----	-----	-.0010	.0095	-----	6.48



TABLE III.—FAIRED VALUES FOR NOSE 6, PROPELLER C—Continued

$V/nD$	Set 35° at 0.75R				Set 40° at 0.75R				Set 45° at 0.75R			
	$C_T$	$C_P$	$\eta$	$C_S$	$C_T$	$C_P$	$\eta$	$C_S$	$C_T$	$C_P$	$\eta$	$C_S$
0	0	0	0	0	0	0	0	0	0	0	0	0
.05	.1770	.2728	.033	.06	.1725	.3324	.026	.06	.1663	.3937	.021	.06
.10	.1757	.2699	.065	.13	.1730	.3320	.052	.12	.1670	.3925	.043	.12
.15	.1723	.2665	.097	.20	.1733	.3313	.079	.19	.1677	.3911	.064	.18
.20	.1702	.2630	.130	.26	.1737	.3302	.105	.25	.1682	.3900	.086	.24
.25	.1680	.2592	.162	.33	.1738	.3288	.132	.31	.1687	.3886	.109	.30
.30	.1659	.2552	.195	.39	.1739	.3270	.160	.38	.1692	.3871	.131	.36
.35	.1638	.2510	.228	.46	.1738	.3249	.187	.44	.1697	.3857	.154	.42
.40	.1618	.2467	.262	.53	.1737	.3226	.215	.50	.1700	.3840	.177	.48
.45	.1600	.2422	.297	.60	.1733	.3199	.244	.57	.1702	.3824	.200	.55
.50	.1582	.2377	.335	.67	.1728	.3170	.273	.63	.1704	.3806	.224	.61
.55	.1566	.2330	.370	.74	.1720	.3138	.302	.69	.1705	.3788	.247	.67
.60	.1550	.2283	.407	.81	.1710	.3102	.330	.76	.1704	.3767	.271	.73
.65	.1538	.2245	.445	.88	.1699	.3066	.360	.82	.1702	.3743	.295	.79
.70	.1527	.2220	.480	.95	.1684	.3027	.388	.89	.1700	.3720	.320	.85
.75	.1517	.2206	.516	1.02	.1663	.2988	.417	.96	.1694	.3690	.344	.92
.80	.1508	.2186	.552	1.09	.1641	.2945	.445	1.02	.1687	.3660	.369	.98
.85	.1501	.2154	.593	1.16	.1619	.2898	.477	1.09	.1678	.3625	.393	1.04
.90	.1488	.2110	.635	1.23	.1598	.2847	.505	1.16	.1666	.3587	.418	1.10
.95	.1471	.2062	.680	1.30	.1578	.2799	.536	1.23	.1650	.3544	.442	1.17
1.00	.1442	.2015	.715	1.38	.1560	.2755	.568	1.30	.1631	.3498	.467	1.24
1.05	.1393	.1968	.743	1.45	.1545	.2712	.599	1.37	.1609	.3446	.490	1.30
1.10	.1340	.1915	.770	1.53	.1531	.2672	.631	1.43	.1585	.3390	.514	1.37
1.15	.1279	.1858	.791	1.61	.1520	.2632	.665	1.50	.1563	.3333	.540	1.43
1.20	.1210	.1795	.810	1.69	.1511	.2595	.699	1.57	.1542	.3280	.564	1.50
1.25	.1131	.1723	.821	1.78	.1497	.2560	.730	1.64	.1522	.3236	.589	1.57
1.30	.1048	.1644	.828	1.87	.1472	.2519	.761	1.71	.1503	.3199	.611	1.63
1.35	.0962	.1550	.837	1.96	.1427	.2470	.780	1.79	.1488	.3168	.633	1.70
1.40	.0875	.1453	.843	2.06	.1372	.2409	.797	1.86	.1476	.3142	.657	1.77
1.45	.0788	.1345	.848	2.17	.1310	.2340	.811	1.94	.1470	.3127	.681	1.83
1.50	.0700	.1236	.850	2.28	.1240	.2262	.822	2.02	.1468	.3110	.708	1.90
1.55	.0611	.1110	.853	2.41	.1160	.2170	.829	2.10	.1460	.3088	.732	1.96
1.60	.0521	.0984	.848	2.54	.1078	.2065	.835	2.19	.1445	.3054	.756	2.03
1.65	.0430	.0843	.842	2.71	.0988	.1950	.836	2.29	.1413	.3010	.775	2.10
1.70	.0340	.0693	.835	2.90	.0900	.1825	.838	2.39	.1370	.2950	.790	2.17
1.75	.0243	.0531	.800	3.15	.0810	.1690	.839	2.49	.1318	.2880	.800	2.25
1.80	.0145	.0365	.715	3.49	.0720	.1540	.840	2.62	.1255	.2800	.806	2.33
1.85	.0048	.0200	.444	4.05	.0630	.1385	.841	2.75	.1191	.2720	.810	2.40
1.90	-.0051	.0031	-----	6.03	.0540	.1230	.835	2.90	.1125	.2636	.811	2.48
1.95	-----	-----	-----	-----	.0450	.1070	.820	3.05	.1056	.2535	.812	2.56
2.00	-----	-----	-----	-----	.0360	.0900	.800	3.24	.0986	.2427	.813	2.66
2.05	-----	-----	-----	-----	.0265	.0720	.754	3.48	.0910	.2293	.814	2.76
2.10	-----	-----	-----	-----	.0175	.0545	.675	3.76	.0830	.2133	.816	2.86
2.15	-----	-----	-----	-----	.0083	.0365	.489	4.16	.0746	.1961	.818	2.98
2.20	-----	-----	-----	-----	-.0008	.0190	-----	4.86	.0663	.1780	.819	3.10
2.25	-----	-----	-----	-----	-.0100	.0010	-----	8.96	.0580	.1595	.820	3.25
2.30	-----	-----	-----	-----	-----	-----	-----	-----	.0500	.1410	.816	3.40
2.35	-----	-----	-----	-----	-----	-----	-----	-----	.0412	.1220	.795	3.58
2.40	-----	-----	-----	-----	-----	-----	-----	-----	.0330	.1040	.762	3.77
2.45	-----	-----	-----	-----	-----	-----	-----	-----	.0242	.0855	.694	4.00
2.50	-----	-----	-----	-----	-----	-----	-----	-----	.0160	.0670	.597	4.26
2.55	-----	-----	-----	-----	-----	-----	-----	-----	.0073	.0485	.383	4.67
2.60	-----	-----	-----	-----	-----	-----	-----	-----	-.0010	.0300	-----	5.24
2.65	-----	-----	-----	-----	-----	-----	-----	-----	-.0065	.0120	-----	6.42



Positive directions of axes and angles (forces and moments) are shown by arrows

Axis		Force (parallel to axis) symbol	Moment about axis			Angle		Velocities	
Designation	Sym- bol		Designation	Sym- bol	Positive direction	Designa- tion	Sym- bol	Linear (compo- nent along axis)	Angular
Longitudinal.....	X	X	Rolling.....	L	Y → Z	Roll.....	φ	u	p
Lateral.....	Y	Y	Pitching.....	M	Z → X	Pitch.....	θ	v	q
Normal.....	Z	Z	Yawing.....	N	X → Y	Yaw.....	ψ	w	r

Absolute coefficients of moment

$$C_l = \frac{L}{qbS}$$

(rolling)

$$C_m = \frac{M}{qcS}$$

(pitching)

$$C_n = \frac{N}{qbS}$$

(yawing)

Angle of set of control surface (relative to neutral position),  $\delta$ . (Indicate surface by proper subscript.)

#### 4. PROPELLER SYMBOLS

$D$ , Diameter

$p$ , Geometric pitch

$p/D$ , Pitch ratio

$V'$ , Inflow velocity

$V_s$ , Slipstream velocity

$T$ , Thrust, absolute coefficient  $C_T = \frac{T}{\rho n^2 D^4}$

$Q$ , Torque, absolute coefficient  $C_Q = \frac{Q}{\rho n^2 D^5}$

$P$ , Power, absolute coefficient  $C_P = \frac{P}{\rho n^3 D^5}$

$C_s$ , Speed-power coefficient  $= \sqrt[5]{\frac{\rho V^5}{P n^2}}$

$\eta$ , Efficiency

$n$ , Revolutions per second, r.p.s.

$\Phi$ , Effective helix angle  $= \tan^{-1}\left(\frac{V}{2\pi r n}\right)$

#### 5. NUMERICAL RELATIONS

1 hp. = 76.04 kg-m/s = 550 ft-lb./sec.

1 metric horsepower = 1.0132 hp.

1 m.p.h. = 0.4470 m.p.s.

1 m.p.s. = 2.2369 m.p.h.

1 lb. = 0.4536 kg.

1 kg = 2.2046 lb.

1 mi. = 1,609.35 m = 5,280 ft.

1 m = 3.2808 ft.

